Optical and Thermal Remote Sensing —— Applications case studies in estuarine, coastal and shelf zones

Shen Fang

Email: fshen@sklec.ecnu.edu.cn

State Key Laboratory of Estuarine and Coastal Research

East China Normal University

Applications in estuarine, coastal and shelf zones

- Sediment dynamics
  - Suspended sediment concentration (SSC)
  - Annual/seasonal/diurnal variation (surface)
  - Vertical variation (SPM transportation model combined)
  - High spatial and temporal resolution
- Phytoplankton dynamics
  - Chlorophyll-a concentration
  - Harmful Algal Blooms (macro- and micro-algae)
  - Phytoplankton size class
  - Phytoplankton species
- Optical and Thermal joint data

Sediment

意义

World: the total amount of sediment entering the sea is 18-24 billion tons/year.

China coasts: accounting for **10% of the total amount** of sediment entering the sea in the world.

From Yellow River and the Yangtze River, account for **about 80% of the total amount** of sediment entering the sea in China.

In the figure, sediment discharge was going to decrease from 1957 to 2007.

Yangtze River Estuary: 100 million tons/year in recent years.

Challenges:

retreat of coastal erosion,

loss of coastal wetlands

and tidal flat resources.

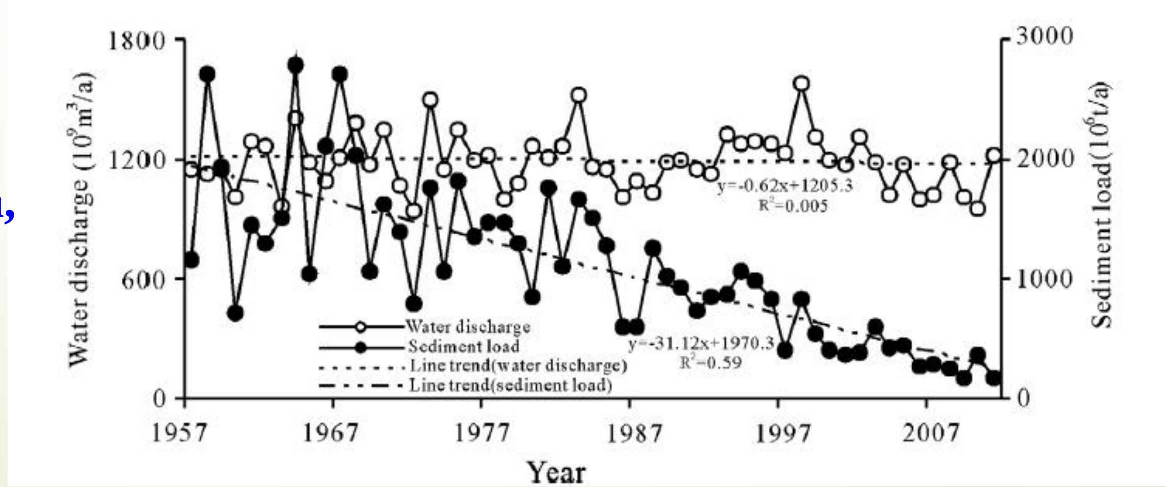

Water discharge and sediment load from the three rivers since the 1950s (Fengliu et al. 2014)

Suspended Sediment 颗粒物的描述

Suspended Sediment：天然水流中所挟带的固体颗粒，悬浮于水中较细的颗粒（极细-粉砂 fine silt <100μm），河口悬沙中值粒径：5μm

Suspended Particulate Matter

Suspended Solid/inorganic minerals

Non-algal particle: 非藻类颗粒物

Tripton: 非生物性悬浮物 inorganic particulate matter suspended in waters

Detritus: 有机物碎屑 dead or waste particulate organic material

Background: SSC in the Yangtze

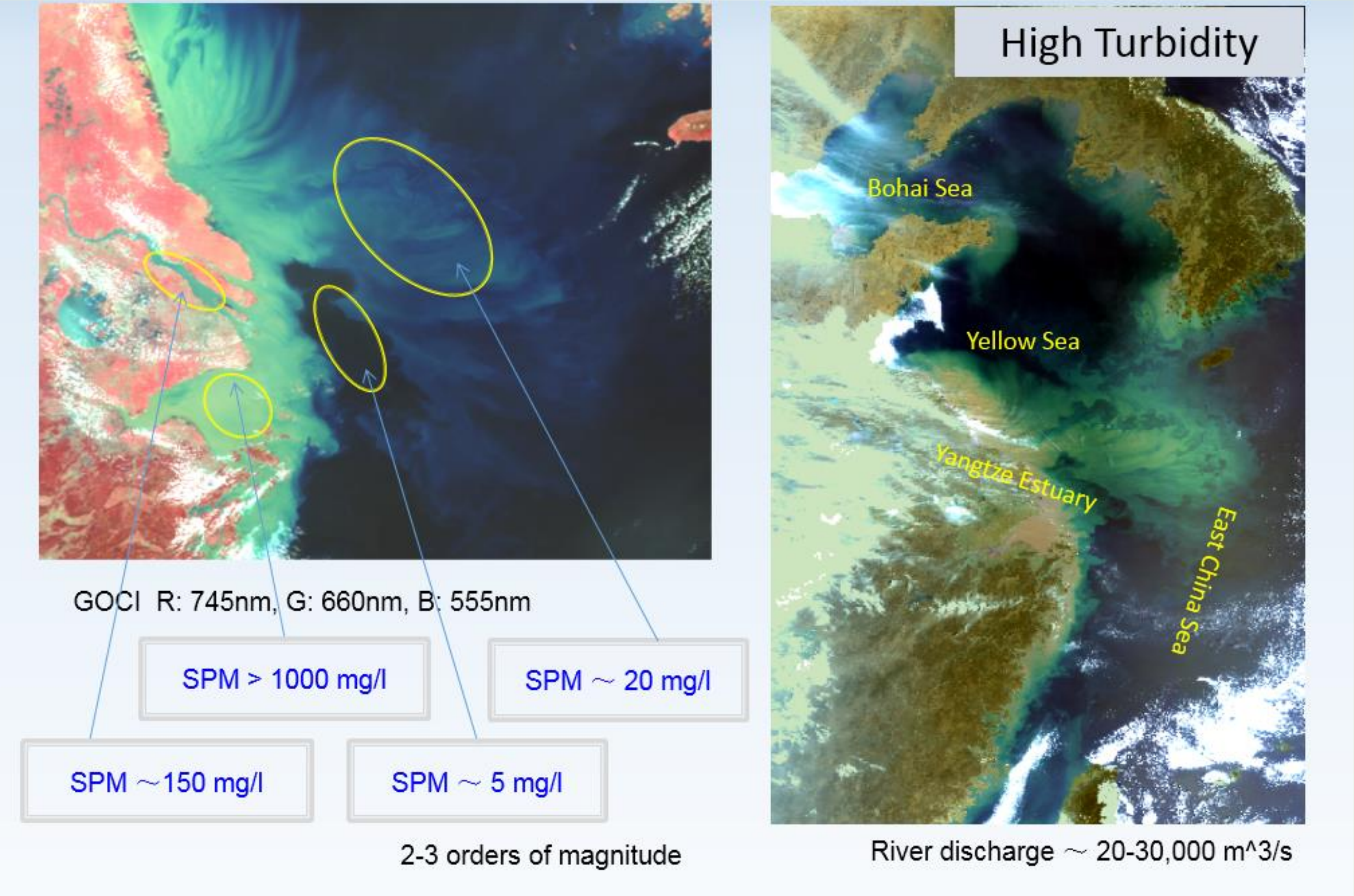

Challenge

低估悬沙浓度、或无效估计

RGB Meris_20100430

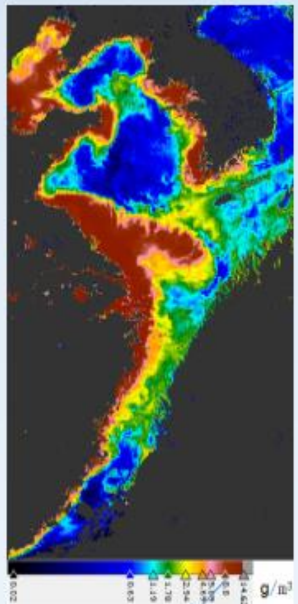

10 mg/L

TSM Meris_20100430

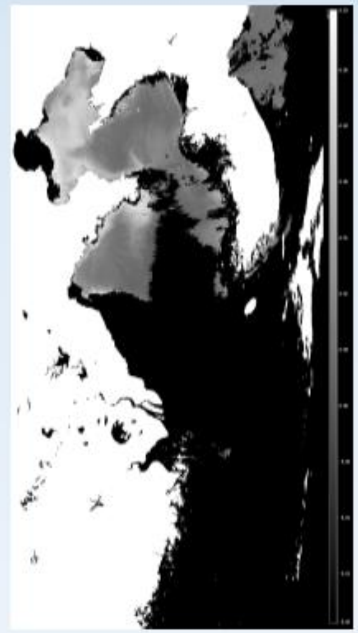

Rrs555nm_MODIS_20100430

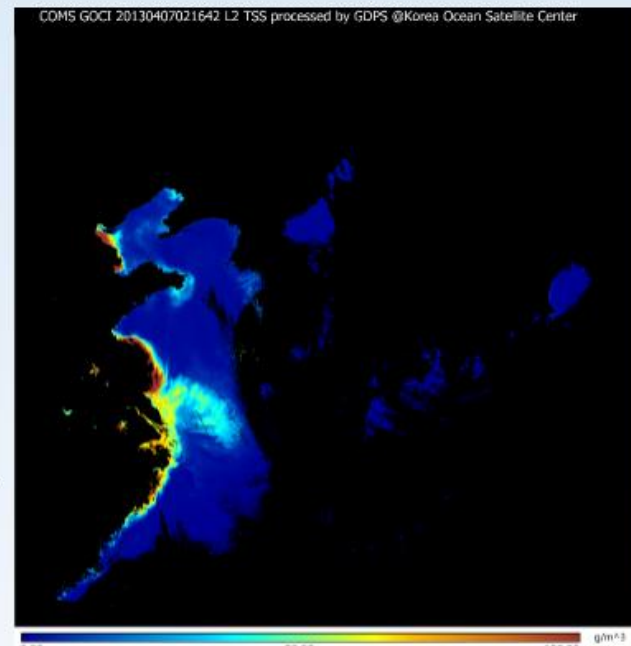

GOCI L2 TSS 20130407

100 mg/L

原因:

- 海洋一类水的算法应用基本失效
- 海洋水色光学反演模型只适用于SSC < 50 mg/l（低浊度水）的海岸水
  不适用于我国近岸水域 >100 mg/l，河口区平均高于500 mg/l

Method: Single band

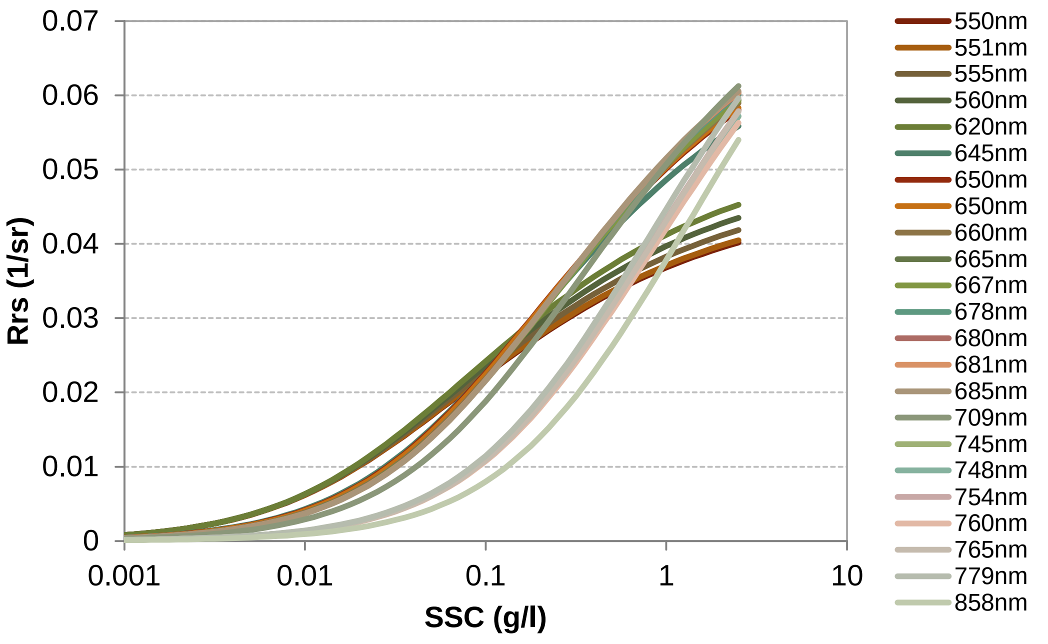

← SERT Model (Shen et al. 2010, 2013)

$$C_{ss} = \frac{(2\alpha / \beta) R_{rs}}{(\alpha - R_{rs})^2}$$

Model from Nechad et al. 2010 ⟶

$$S = A^{\rho} \frac{\rho_w}{1 - \rho_w / C^p} [\mathrm{gm}^{-3}]$$

$$\rho_w(\lambda) = \pi R_{rs}(\lambda)$$

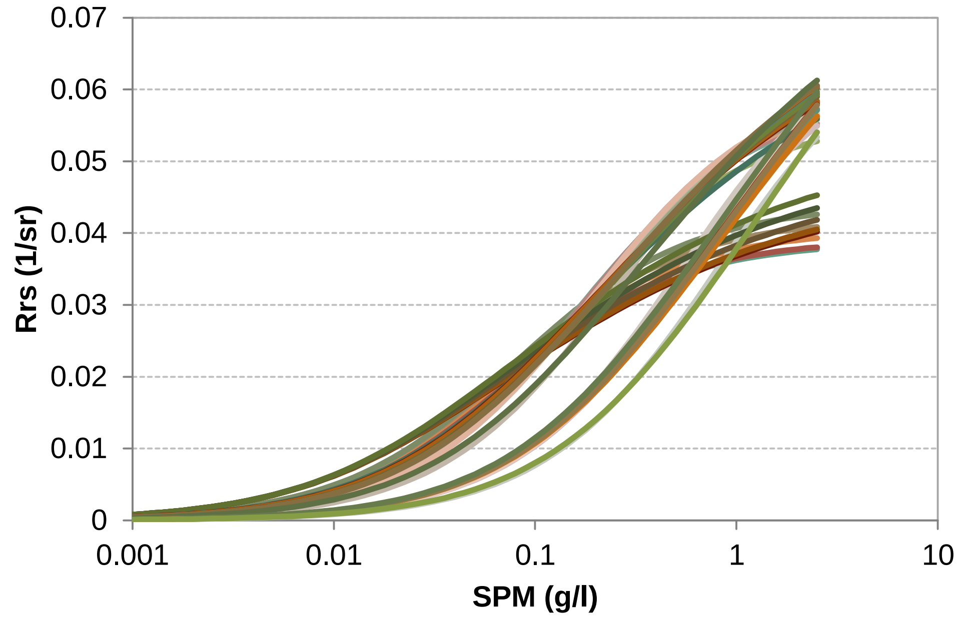

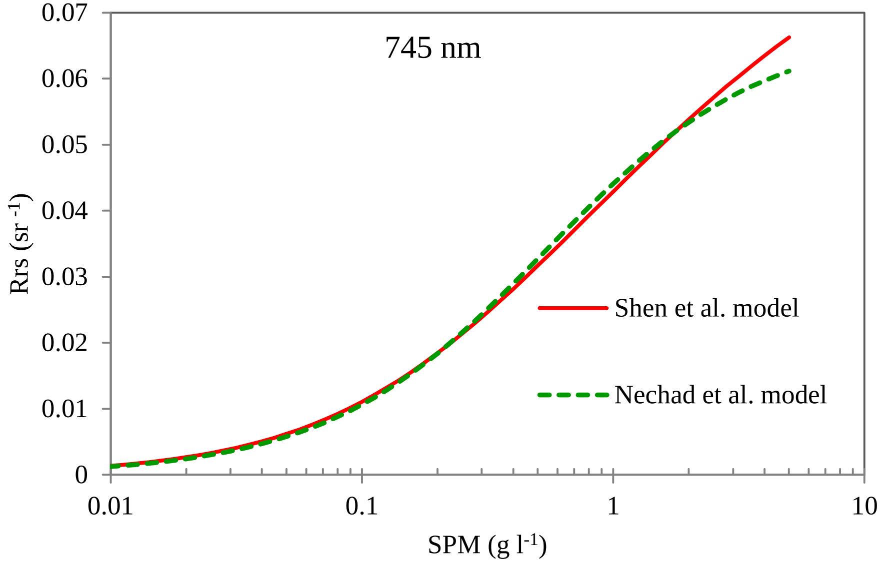

$$S = A^{\rho} \frac{\rho_w}{1 - \rho_w / C^p} \,[\mathrm{gm}^{-3}]$$

$$C_{ss} = \frac{(2\alpha / \beta) R_{rs}}{(\alpha - R_{rs})^2}$$

Method: Bands ratio

$$\mathrm{SPM} = 12.996 \times \exp\left(\frac{\Re_{21}}{0.189}\right)$$

(Doxaran et al. 2010)

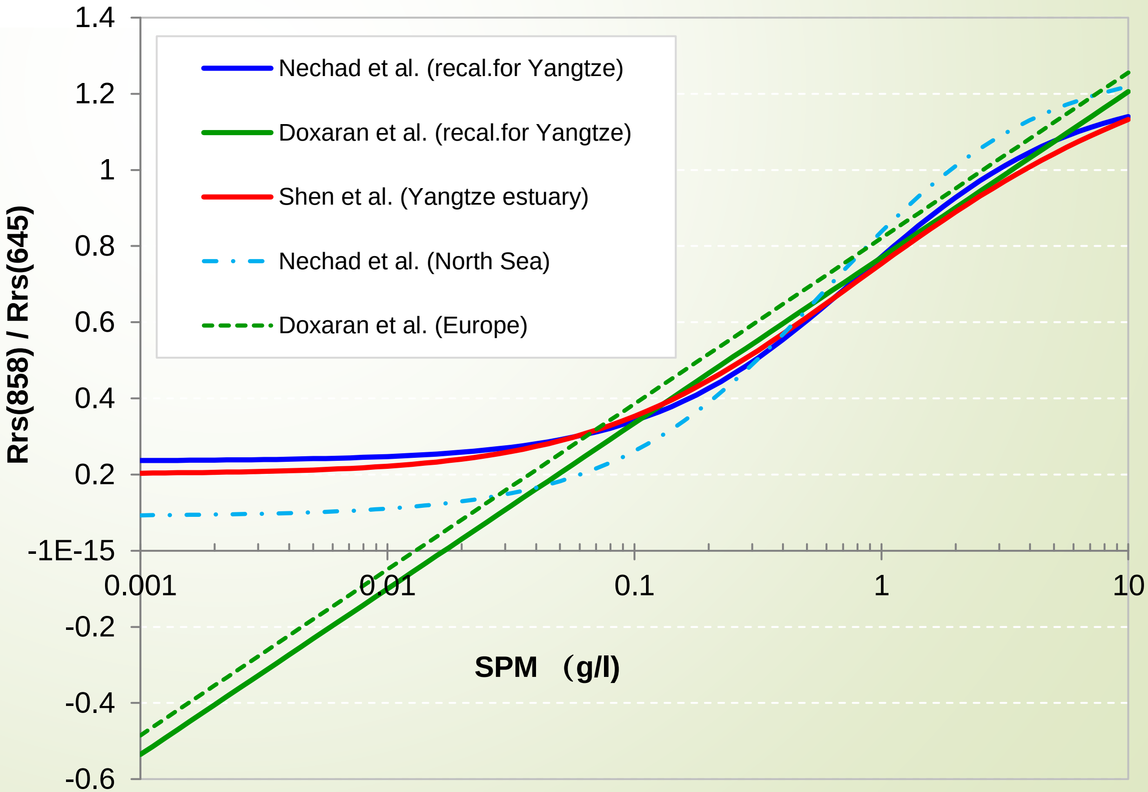

SSC

Calibration & Validation

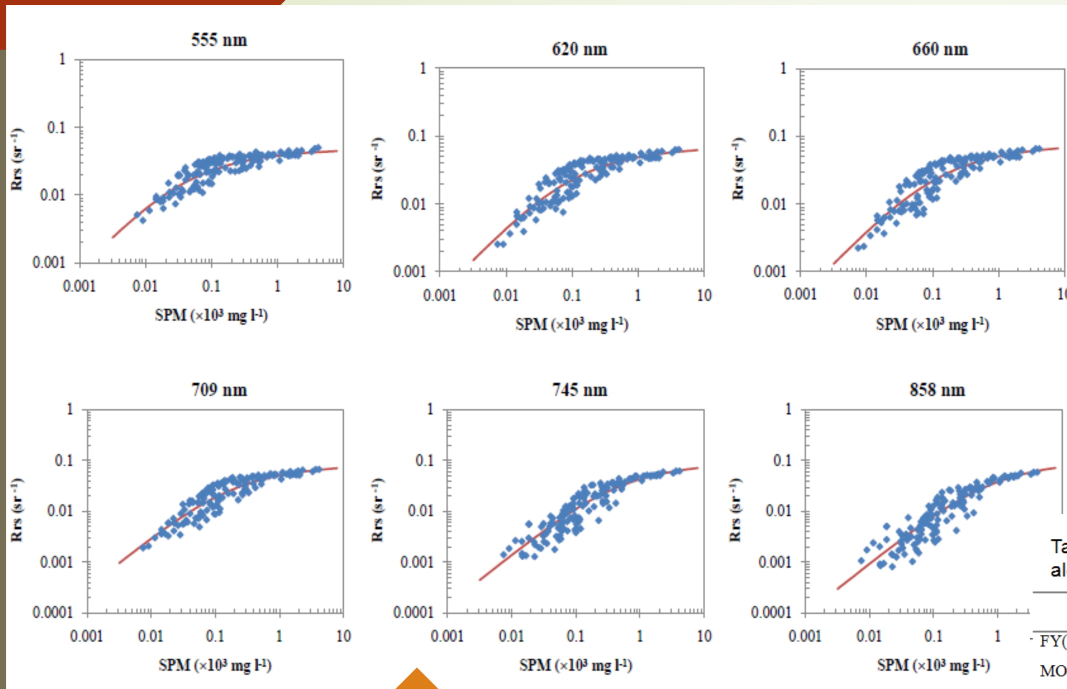

Non-linear regression curve for multi-sensor at 6 candidate bands (555, 620, 660, 709, 745 and 858 nm), with 144 samples of SPM vs. Rrs data on the scatter plot.

(Shen et al. 2014, IJRS)

Recalibrating the SERT model using in situ measurements from 17 cruise campaigns between 2004 and 2012

The recalibrated SERT applied to MODIS, MERIS, GOCI, FY-3/MERSI

Table 2 The α and β coefficients for the MODIS, MERIS, FY-3/MERSI and GOCI SPM algorithms in their spectral bands (> 550 nm) adapted to highly turbid waters.

Sensors	Central bands (nm)	α	β	APD (%)	RMSE(sr^{-1})	R^2 (%)
FY(250)	550nm	0.0467	35.2459	20.2353	0.0057	75.77
MODIS(1km)	551nm	0.0471	34.9441	20.2754	0.0057	75.83
GOCI	555nm	0.0488	33.7132	20.5207	0.0059	75.95
MERIS	560nm	0.0509	32.2256	20.8517	0.0062	76.18
FY(1km)	565nm	0.0532	30.5814	21.1969	0.0064	76.31
MERIS	620nm	0.0711	13.688	26.7349	0.0081	78.22
MODIS(250)	645nm	0.0747	12.4377	27.1824	0.0082	79.12
FY(250)	650nm	0.0754	12.0454	27.4604	0.0082	79.31
GOCI	660nm	0.0771	11.0158	29.2043	0.0084	79.22
MERIS	665nm	0.0779	10.7085	29.9945	0.0085	79.05
MODIS(1km)	667nm	0.0779	10.6286	30.2303	0.0085	79.08
MODIS(1km)	678nm	0.0793	10.3241	29.5631	0.0085	79.58
GOCI	680nm	0.0797	10.2475	29.2608	0.0085	79.85
MERIS	681nm	0.0798	10.2189	29.1862	0.0084	79.89
FY(1km)	685nm	0.0801	10.1105	28.9331	0.0084	80.04
MERIS	709nm	0.0851	7.3001	30.6066	0.0078	83.10
GOCI	745nm	0.0954	2.9698	39.4375	0.0057	89.35
MODIS(1km)	748nm	0.0958	2.9325	39.2503	0.0057	89.48
MERIS	754nm	0.0976	2.8571	38.9281	0.0057	89.71
MERIS	760nm	0.0946	2.8887	39.6762	0.0057	89.10
FY(1km)	765nm	0.0978	2.8182	39.2072	0.0057	89.58
MERIS	779nm	0.0999	2.9285	39.1730	0.0059	89.45
MODIS(250)	858nm	0.1038	1.8042	44.2173	0.0048	91.23

SSC

Calibration & Validation

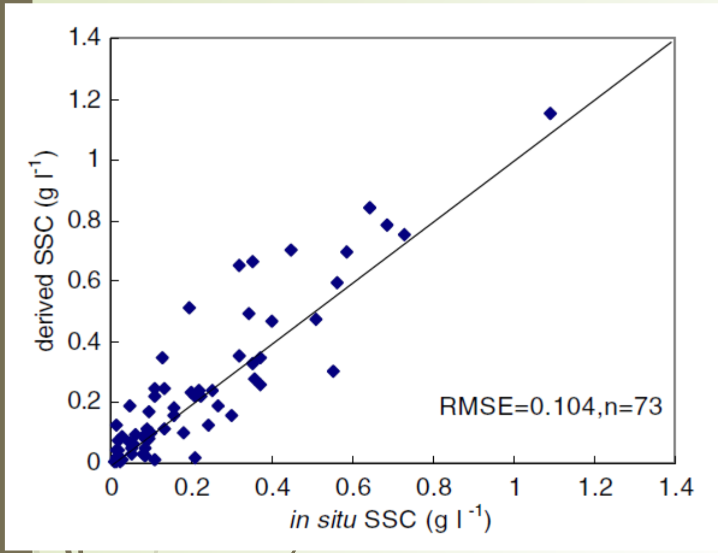

(Shen et al. 2010, E&C)

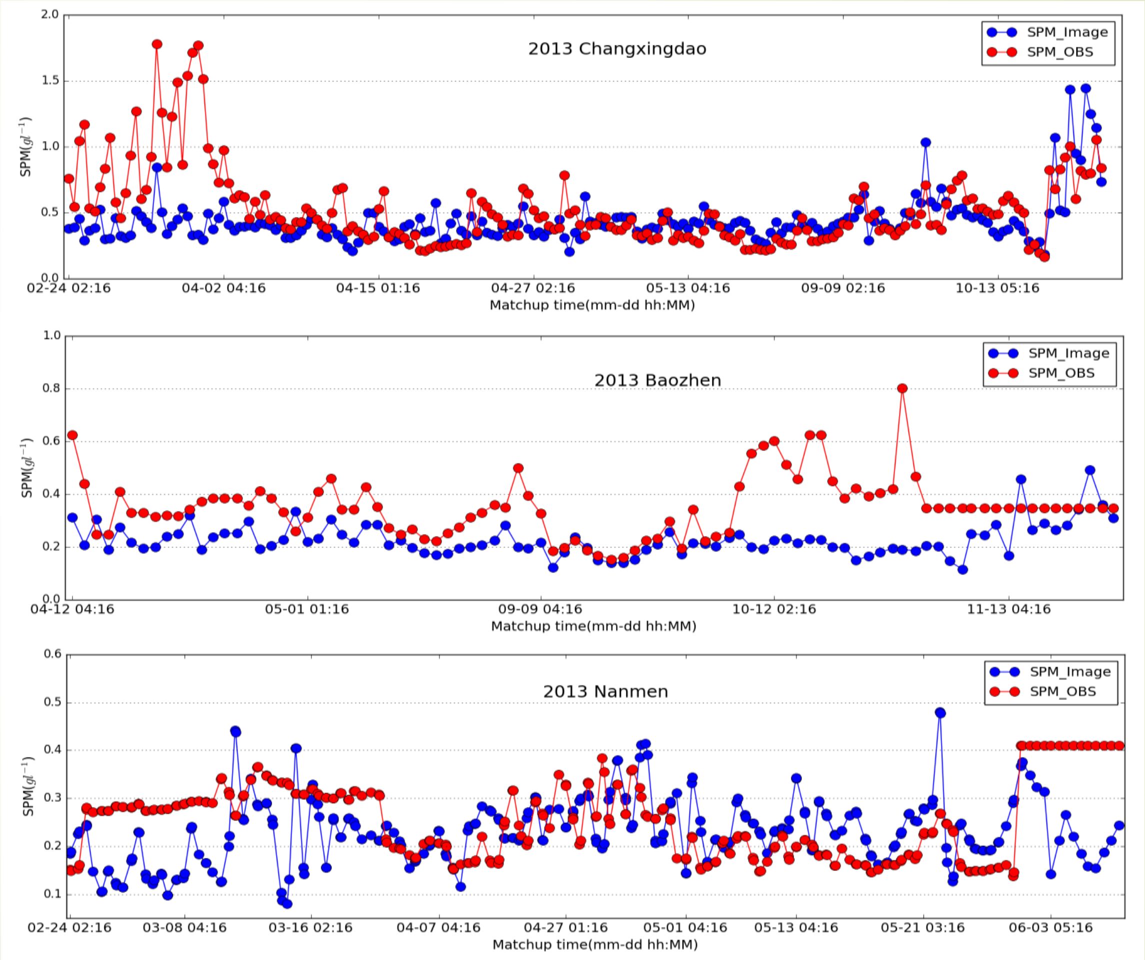

(Pan, Shen & Verhoef 2017, RSE)

Seasonal variation

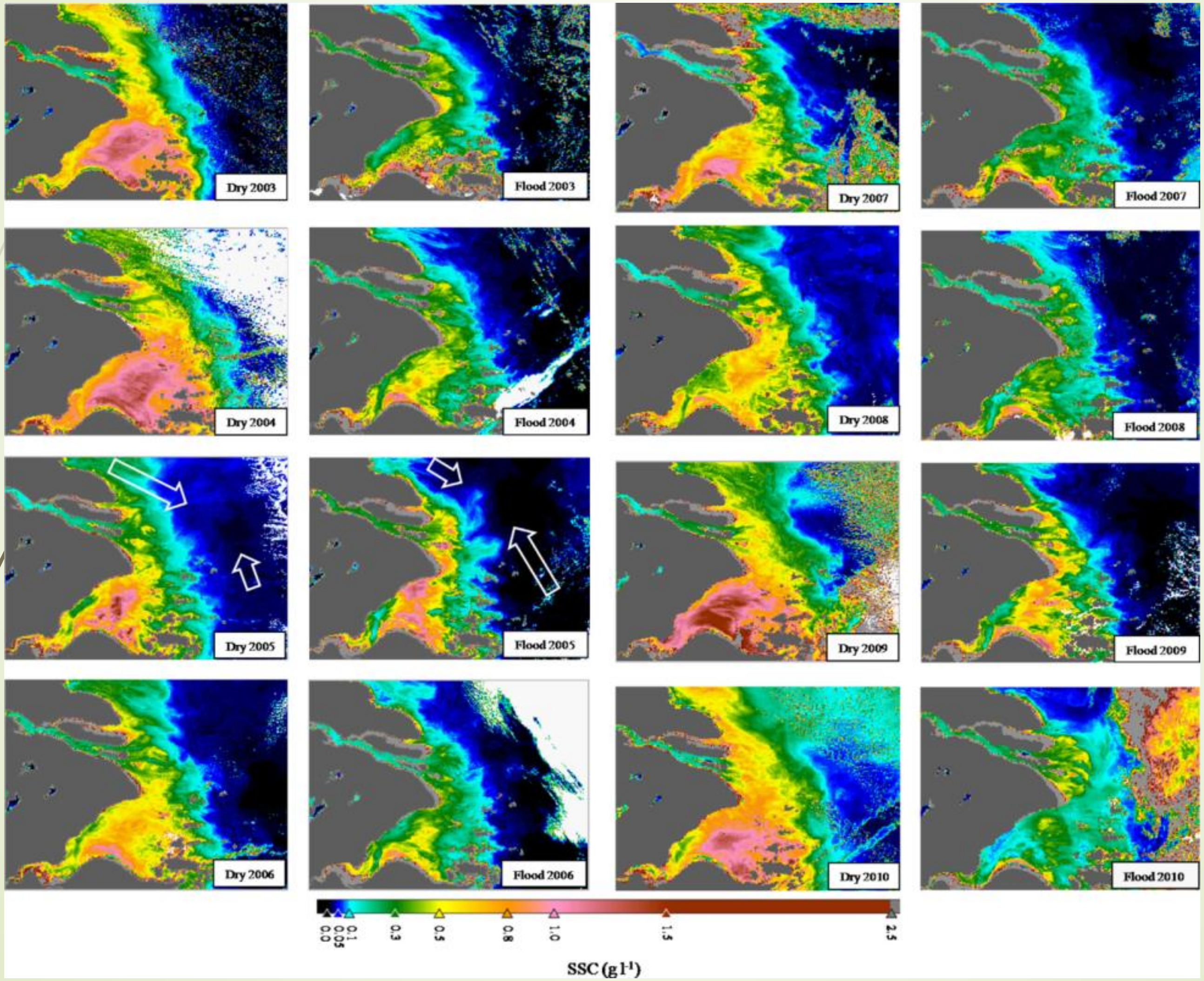

(Shen et al 2013, CSR)

MERIS-derived SPM seasonal composite products from 2003 to 2010

Seasonal variation

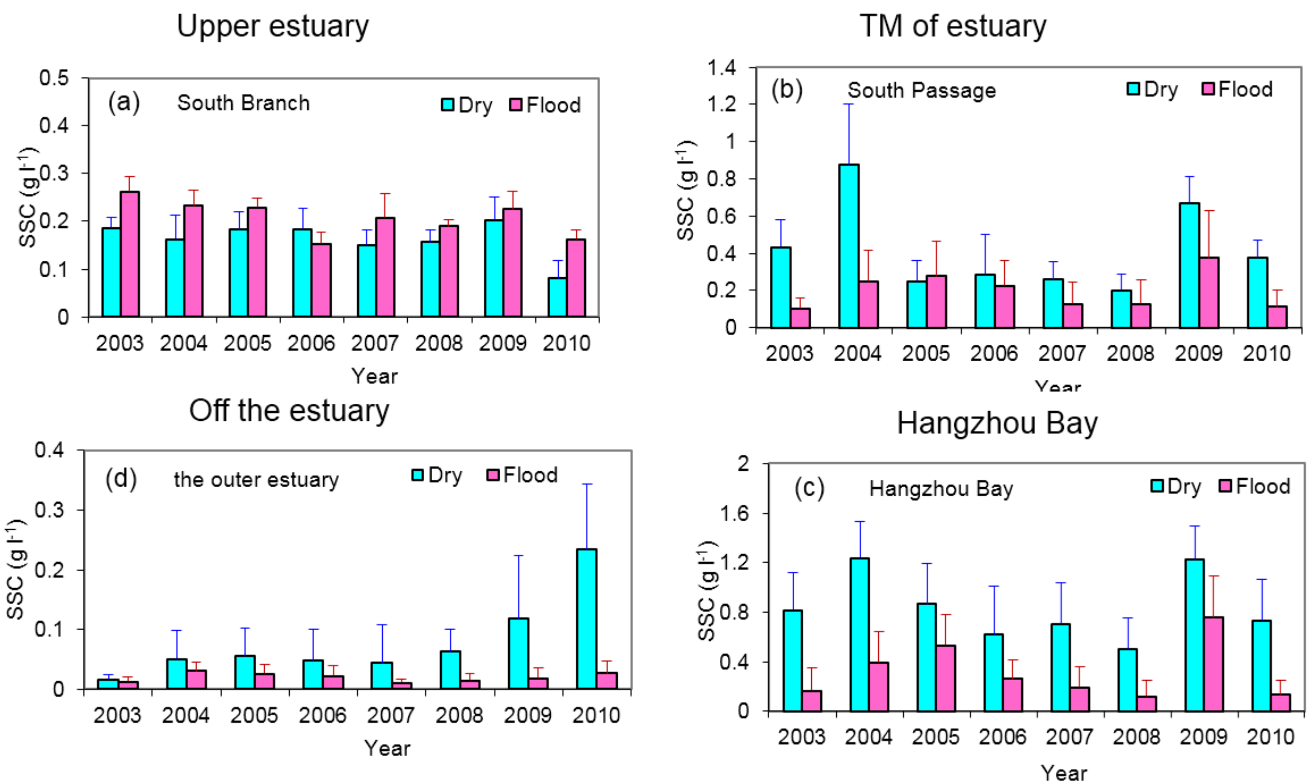

- Seasonal variations
- Annual variations

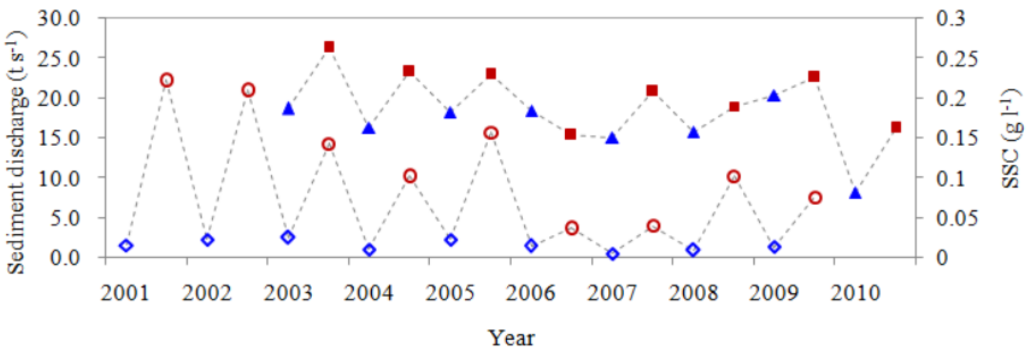

(Shen et al. 2013, CSR)

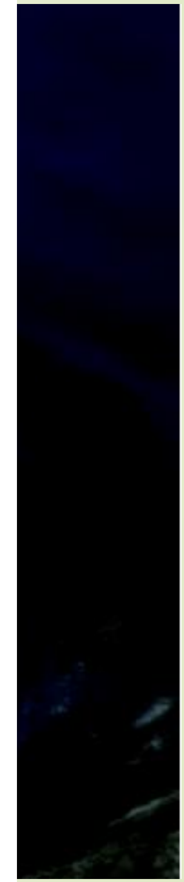

Diurnal variation

涨落潮、日变化

GOCI-derived SSC

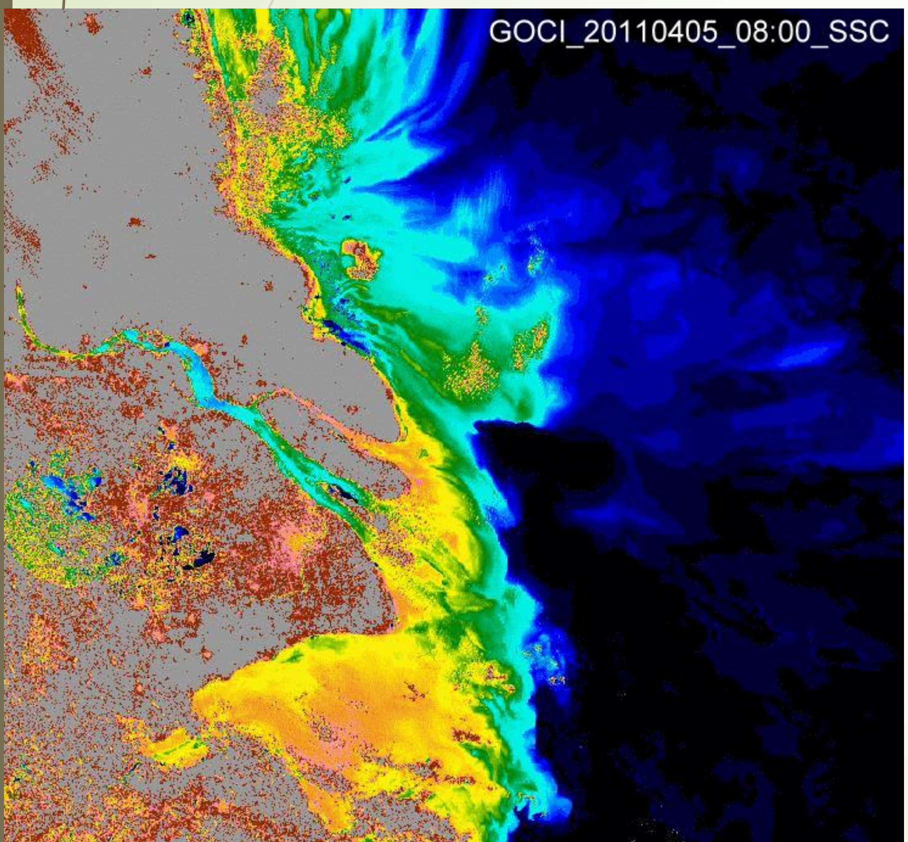

5 April, 2011 in spring tide

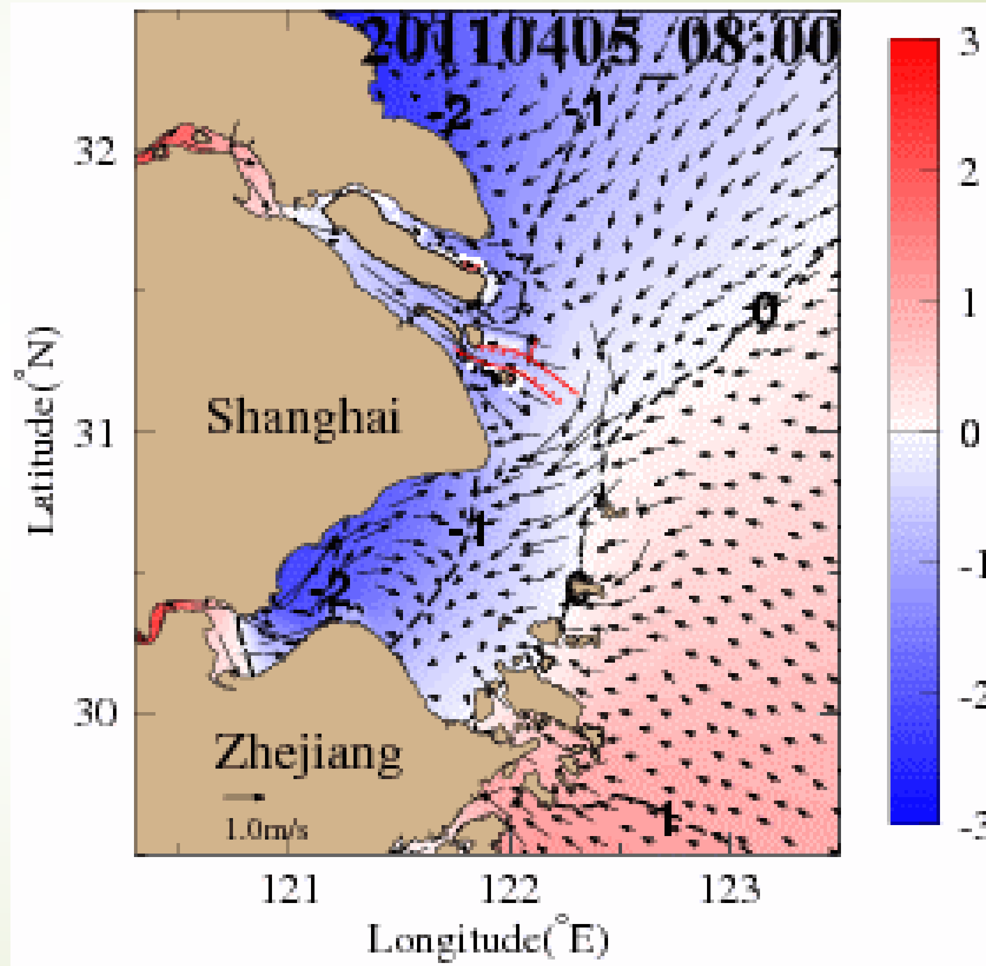

Surface elevation and currents by FVCOM model

SSC vertical variation

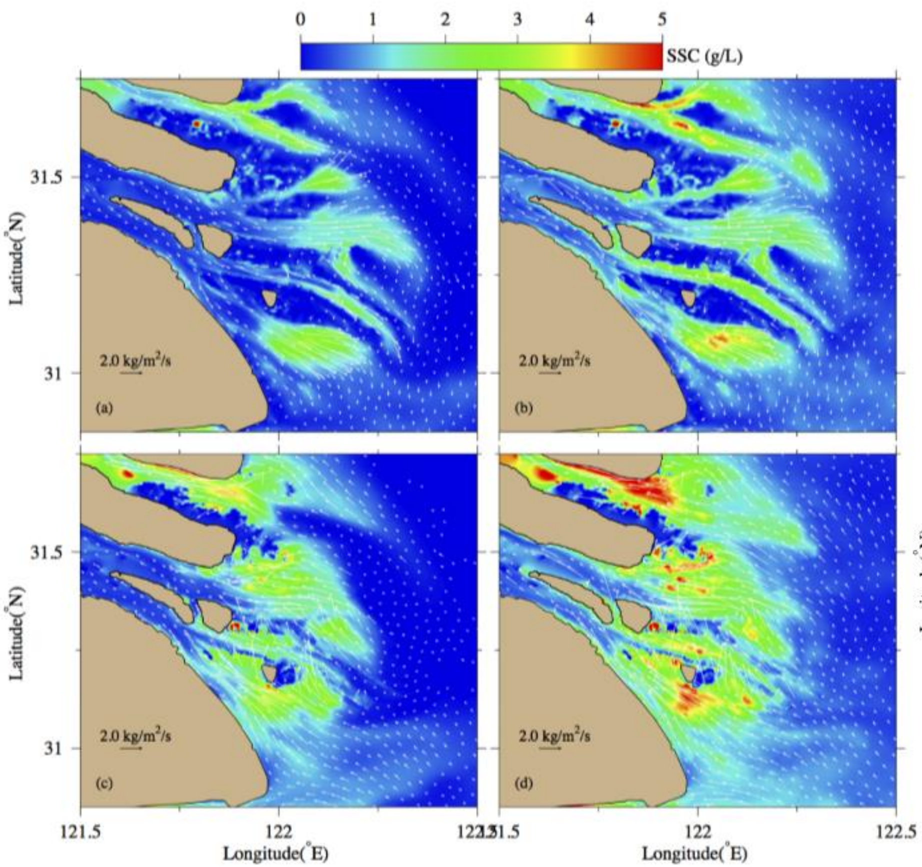

2011年4月大潮 表、底SSC

Ge, J., F. Shen, W. Guo, C. Chen, and P. Ding (2015), Estimation of critical shear stress for erosion in the Changjiang Estuary: A synergy research of observation, GOCI sensing and modeling, ***J. Geophys. Res. Oceans***,120, doi:10.1002/2015JC010992.

GOCI-derived near-bottom critical shear stress

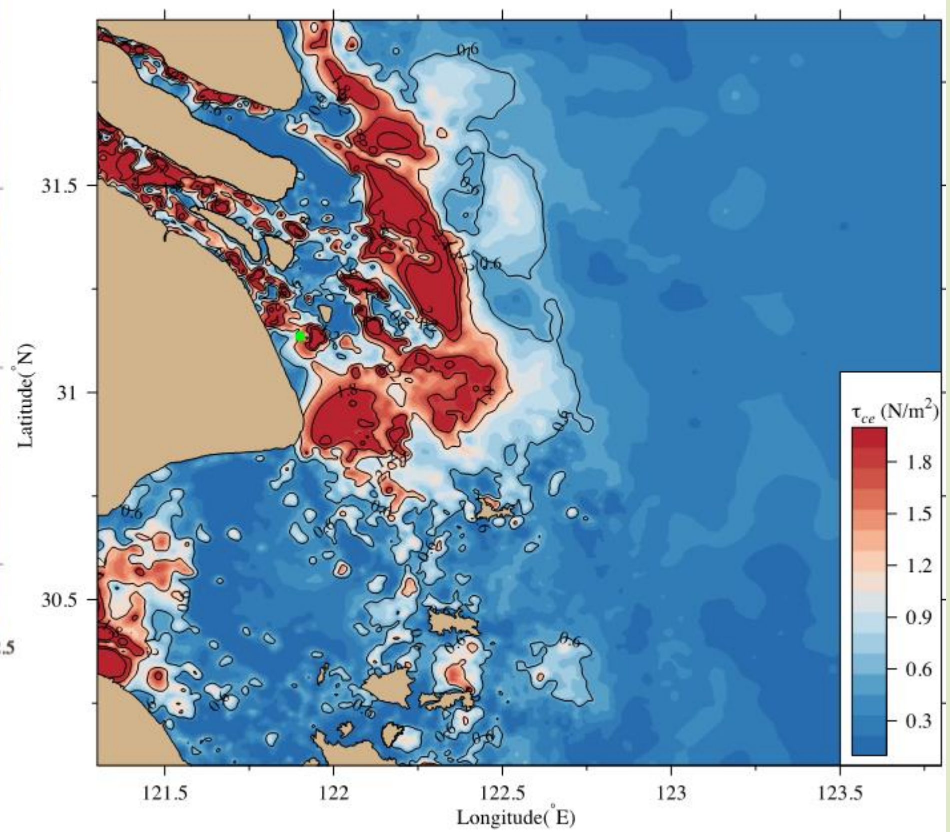

GOCI 反演的近底边界层临界剪切应力 (τ_{ce}) 空间分布

Multi-sensor medium spatial-resolution data for SSC

MERIS vs. GOCI

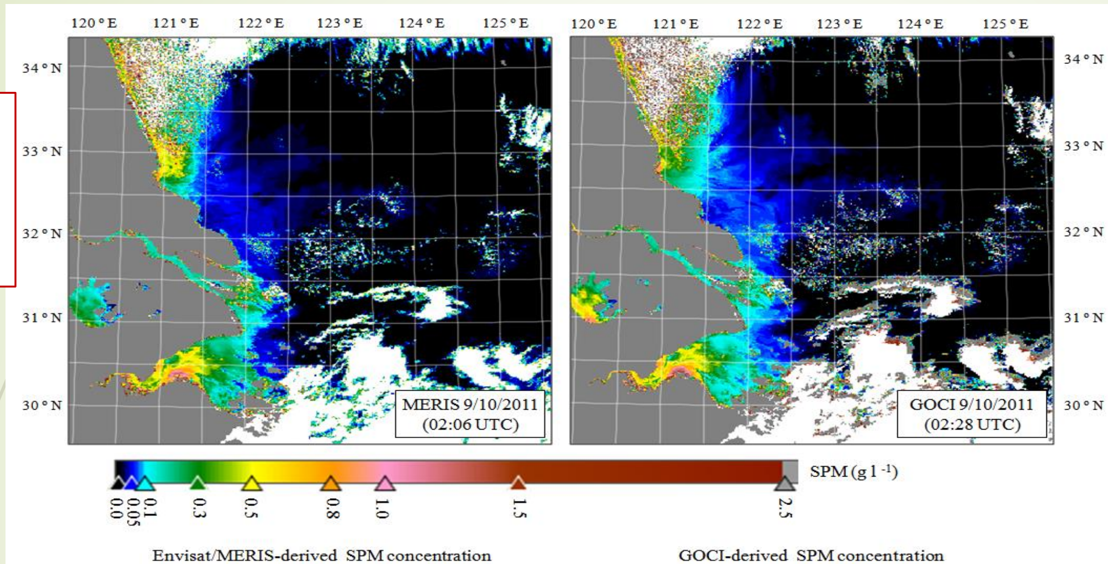

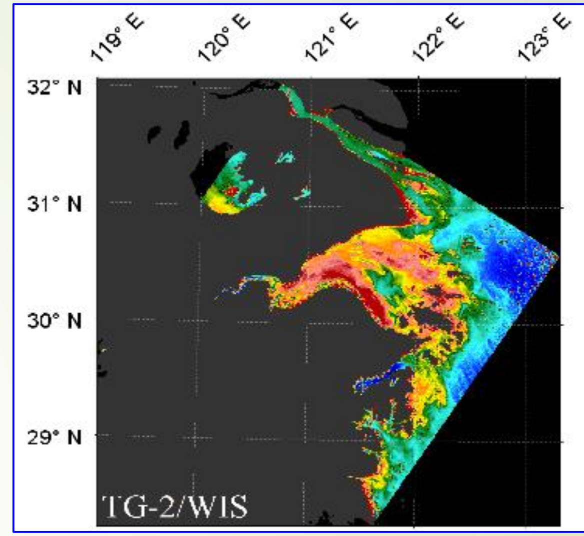

TianGong-2/WIS

MODIS vs. GOCI

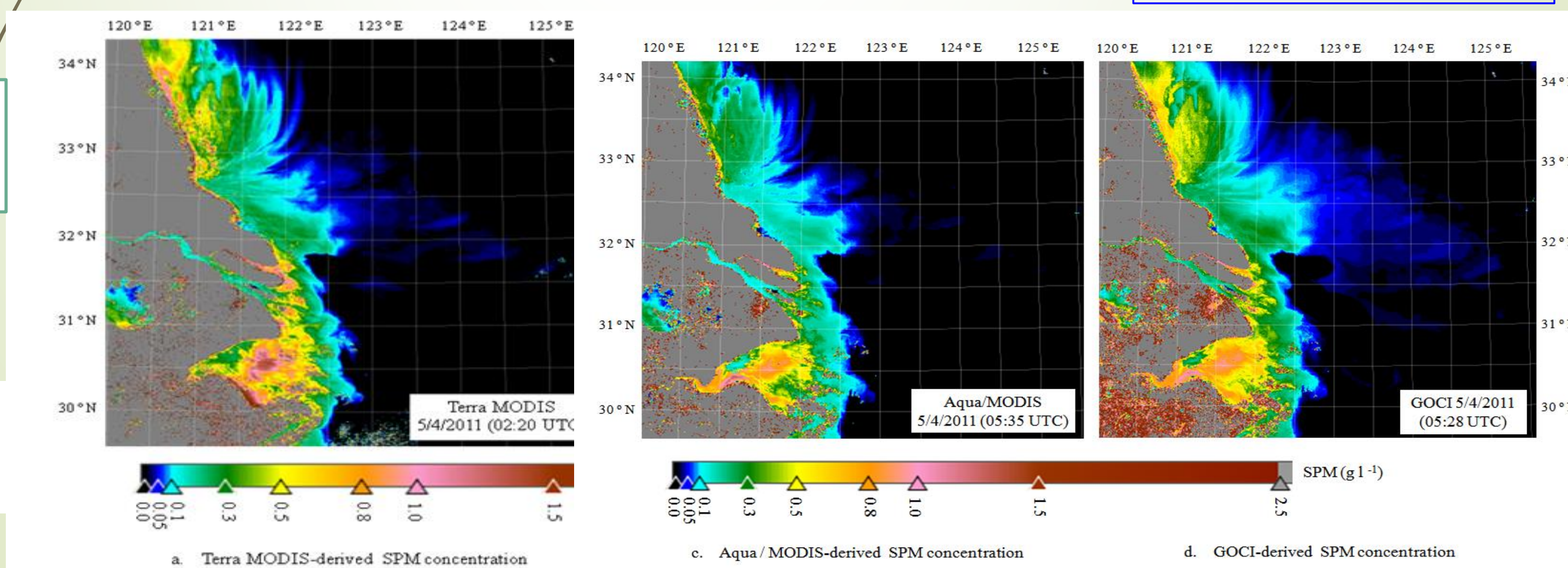

(Shen et al. 2014)

Multi-sensor high spatial-resolution data for SSC

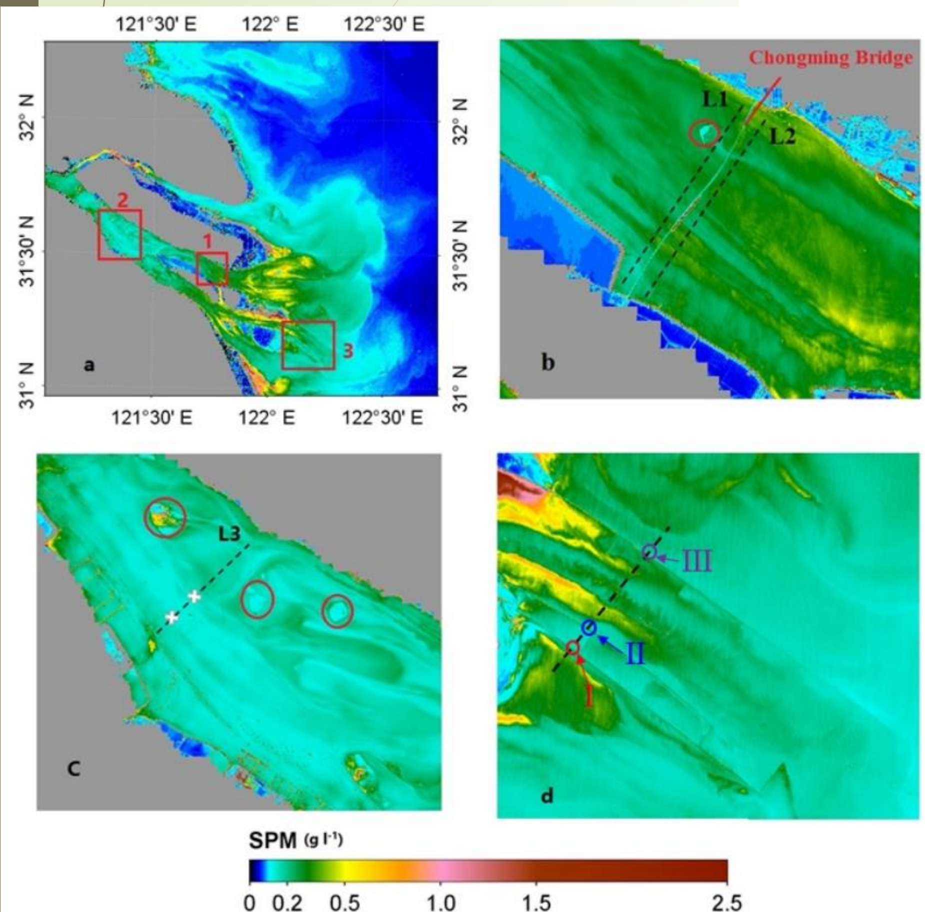

L8/OLI derived SSC

(Pan et al, 2018)

GaoFen-1/WFV derived SSC

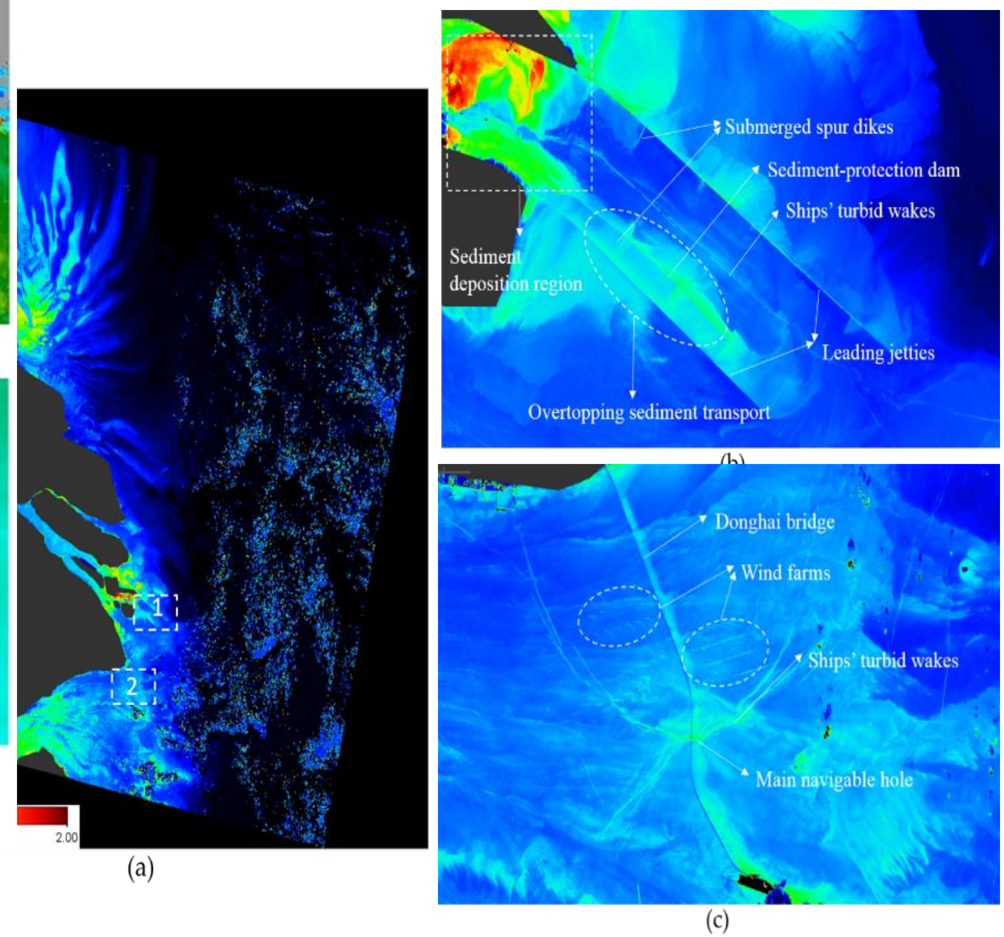

(Shang & Shen, 2016)

Fusion of high spatial and temporal resolution data for SSC

GOCI
500m,
1hr

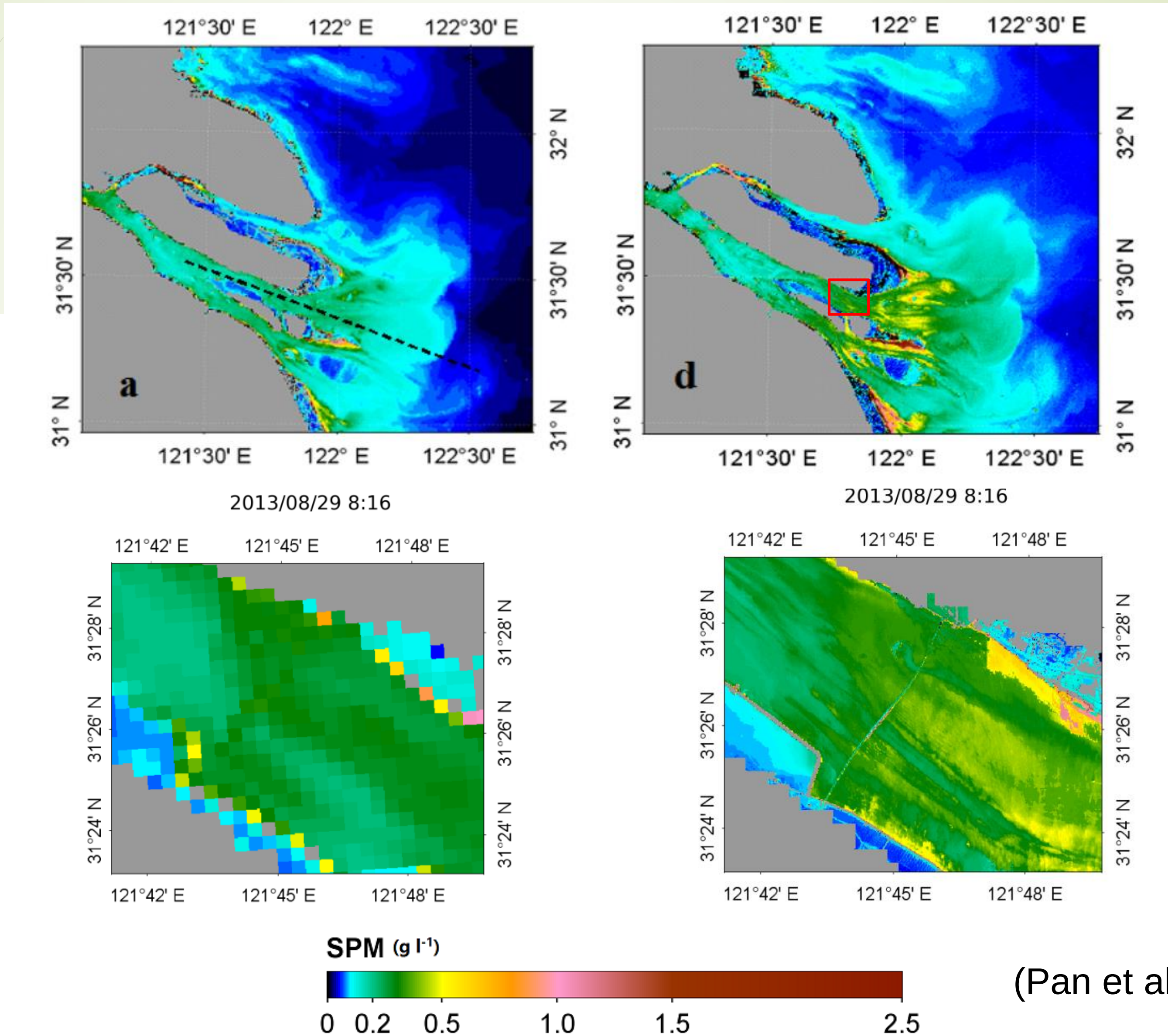

L8/OLI
30m,
16d

(Pan et al, 2018)

High spatial-temporal resolution sediment dynamics

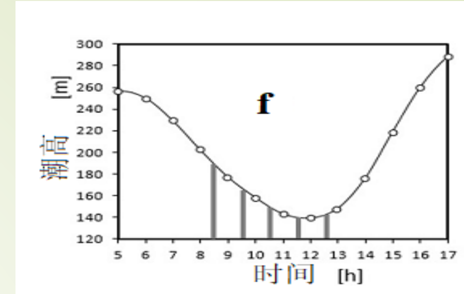

(Pan et al, 2018)

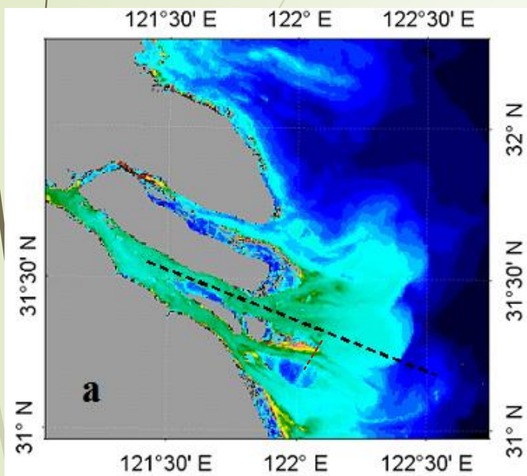

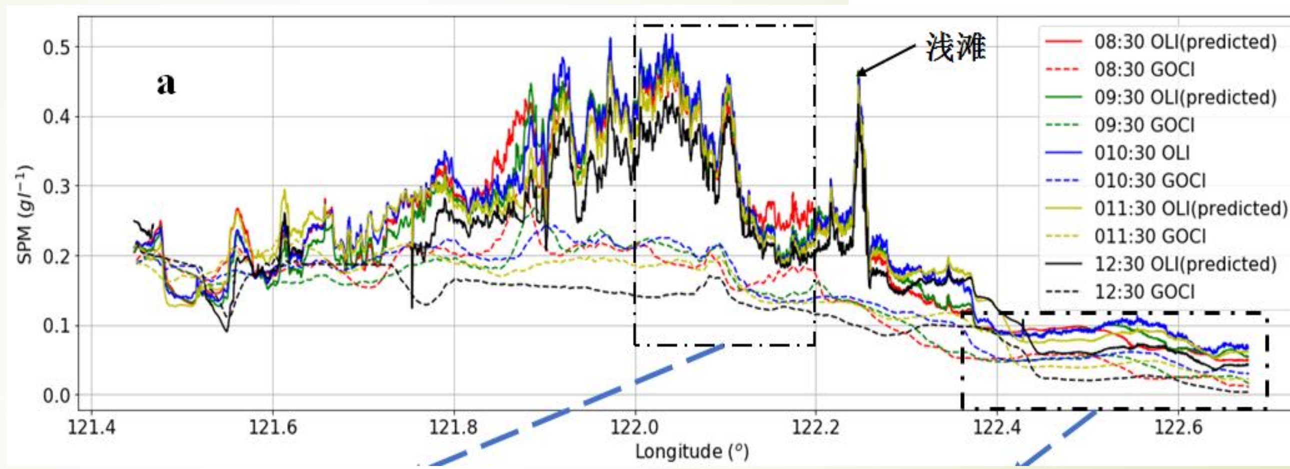

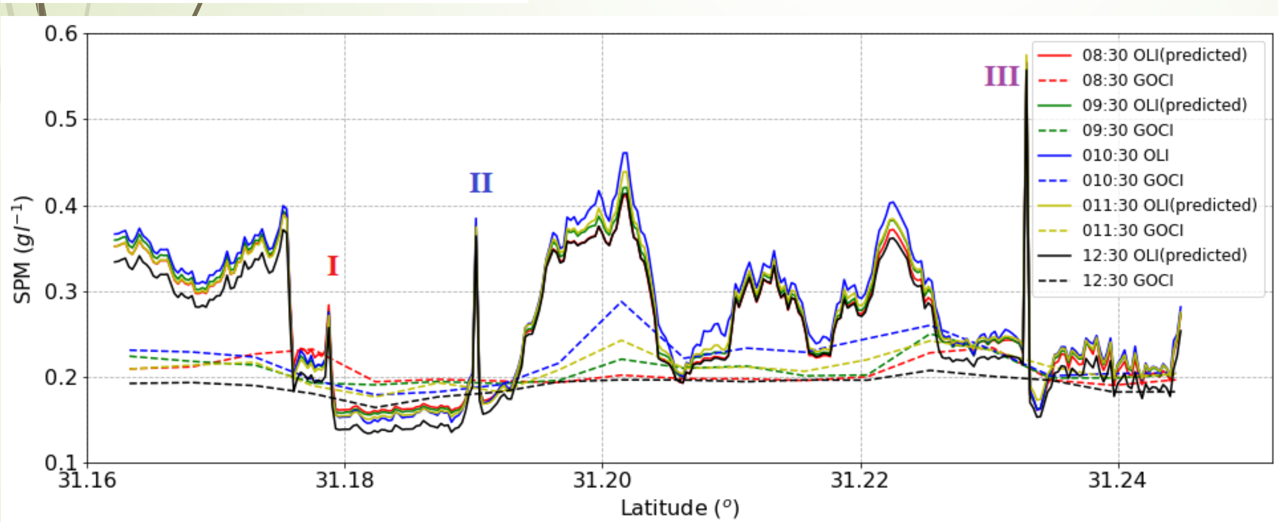

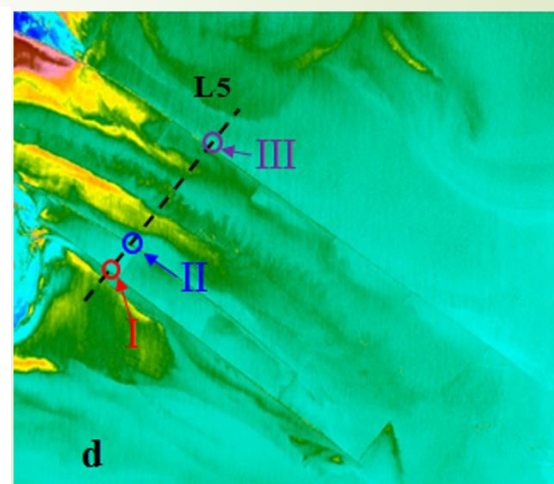

Applications in estuarine, coastal and shelf zones

- Sediment dynamics
  - Suspended sediment concentration (SSC)
  - Annual/seasonal/diurnal variation (surface)
  - Vertical variation (SPM transportation model combined)
  - High spatial and temporal resolution
- Phytoplankton dynamics
  - Chlorophyll-a concentration
  - Harmful Algal Blooms (macro- and micro-algae)
  - Phytoplankton size class
  - Phytoplankton species
- Optical and Thermal joint data

Phytoplankton

- **Phytoplankton** is the base of several aquatic food webs.
- **Phytoplankton** is responsible for most of the transfer of carbon dioxide from the atmosphere to the ocean, and then fixing carbon into organic material, known as primary production.

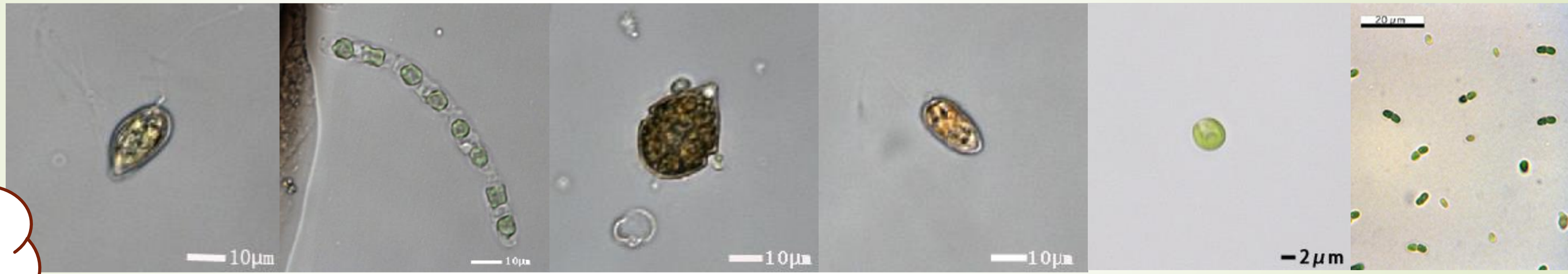

Chl-a as a proxy

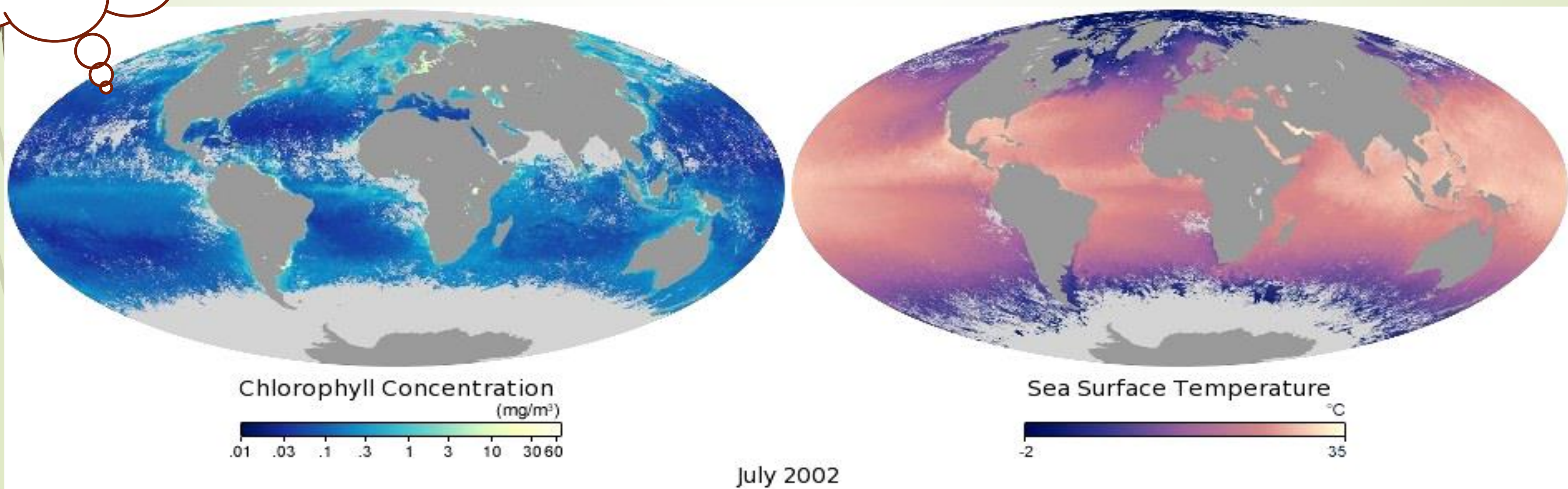

Chlorophyll-a (Chla)

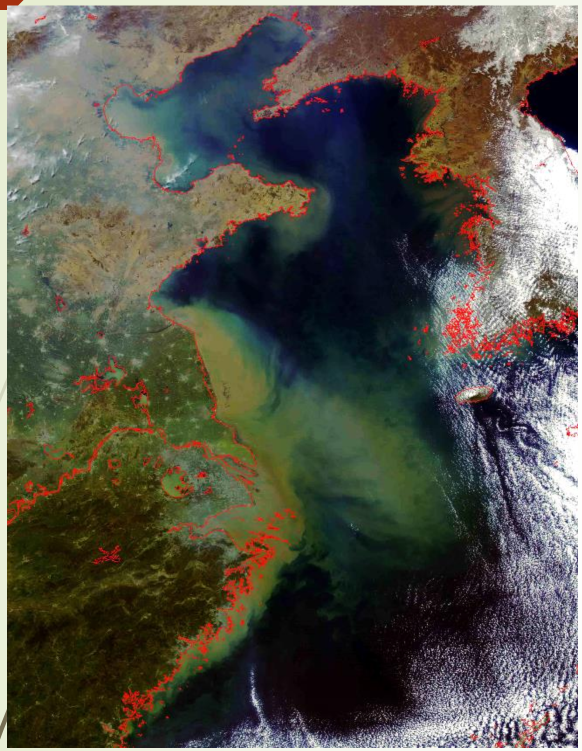

Challenge: sediment-rich waters

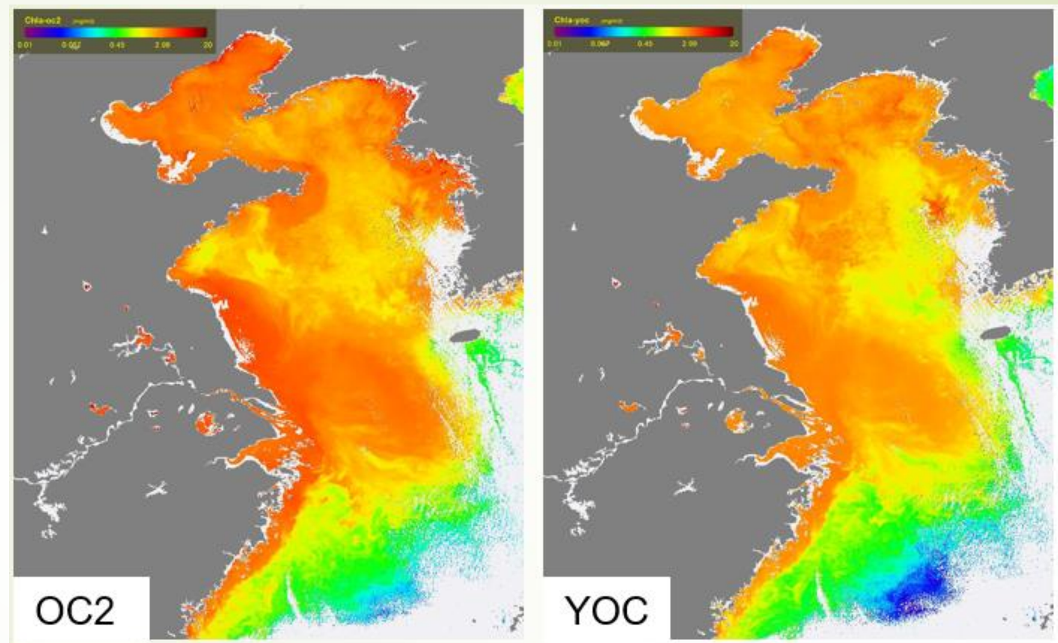

2013年4月7日北京时间12:28

OC2: Ocean Chla algorithm in SeaDAS (O'Reilly et al. 1998)

$$\mathrm{Chla}_{OC2} = e_0 + 10^{e_1+e_2*R+e_3*R^2+e_4*R^3}$$

$$\mathrm{R} = log_{10}\left(\frac{R_{rs}(490)}{R_{rs}(555)}\right)$$

$e_0 = -0.0929$, $e_1 = 0.2974$, $e_2 = -2.2429$,

$e_3 = 0.8358$, $e_4 = -0.0077$

YOC: algorithm for Chla retrieval in the YS and ECS (Siswanto et al., 2011)

$$\text{Chl-}a = 10^{\left(0.342-2.511\ \mathrm{Log}_{10}(R)-0.277\ \mathrm{Log}_{10}^{2}(R)\right)}$$

$$R = \left(\frac{\mathrm{Rrs}_{443}}{\mathrm{Rrs}_{555}}\right)\left(\frac{\mathrm{Rrs}_{412}}{\mathrm{Rrs}_{490}}\right)^{-1.012}.$$

Bands: 412, 442, 490, 555 nm

Chlorophyll-a (Chla)

- Synthetic chlorophyll index (SCI) proposed for Chla retrieval in sediment-rich productive turbid waters, for minimizing the sediment (Shen et al., 2010 IJRS).

$$H_{\mathrm{chl}} = \left[R_{\mathrm{rs}}(\lambda_4) + \frac{\lambda_4 - \lambda_3}{\lambda_4 - \lambda_2} \left(R_{\mathrm{rs}}(\lambda_2) - R_{\mathrm{rs}}(\lambda_4) \right) \right] - R_{\mathrm{rs}}(\lambda_3).$$

$$H_{\Delta} = R_{\mathrm{rs}}(\lambda_2) - \left[R_{\mathrm{rs}}(\lambda_4) + \frac{\lambda_4 - \lambda_2}{\lambda_4 - \lambda_1} \left(R_{\mathrm{rs}}(\lambda_1) - R_{\mathrm{rs}}(\lambda_4) \right) \right].$$

$$\mathrm{SCI} = H_{\mathrm{chl}} - H_{\Delta}.$$

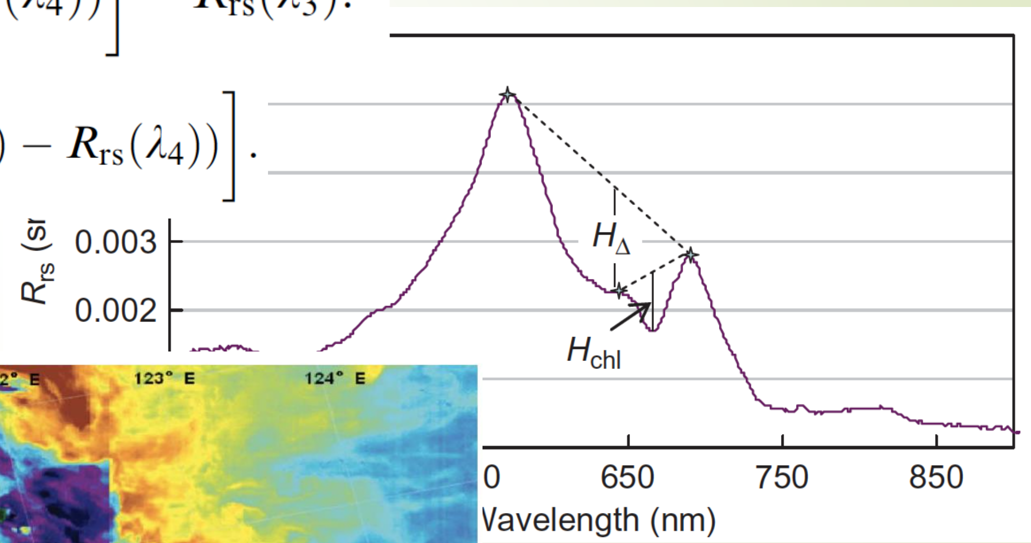

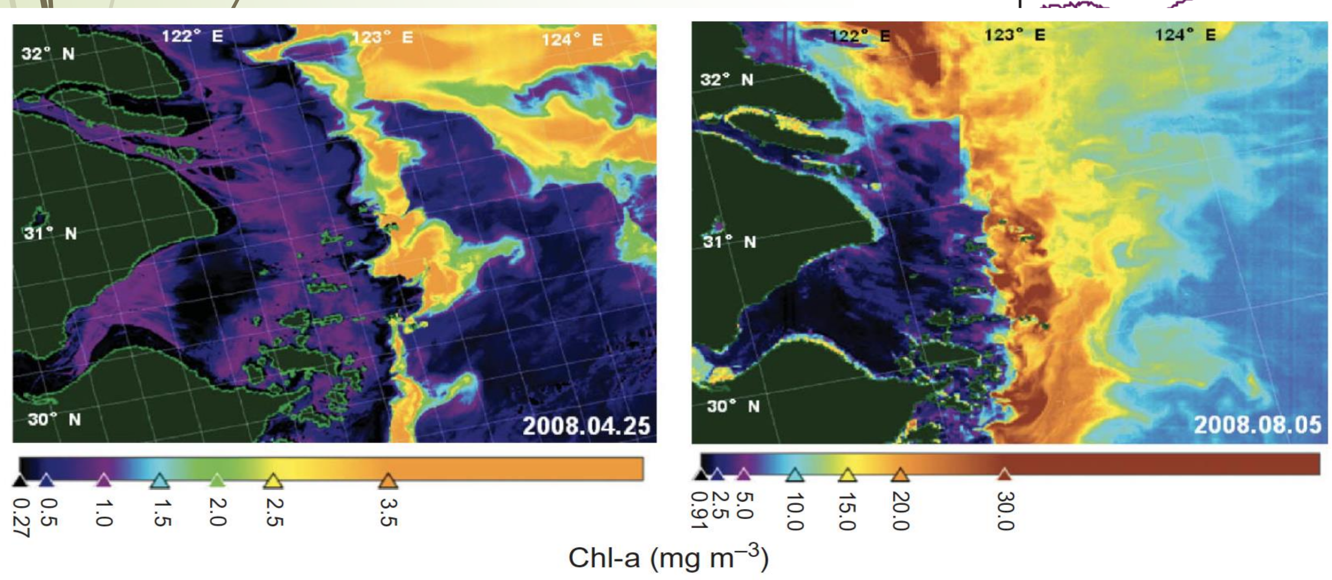

Bands:
560,620,665,709 nm

MERIS-derived Chla by the SCI algorithm

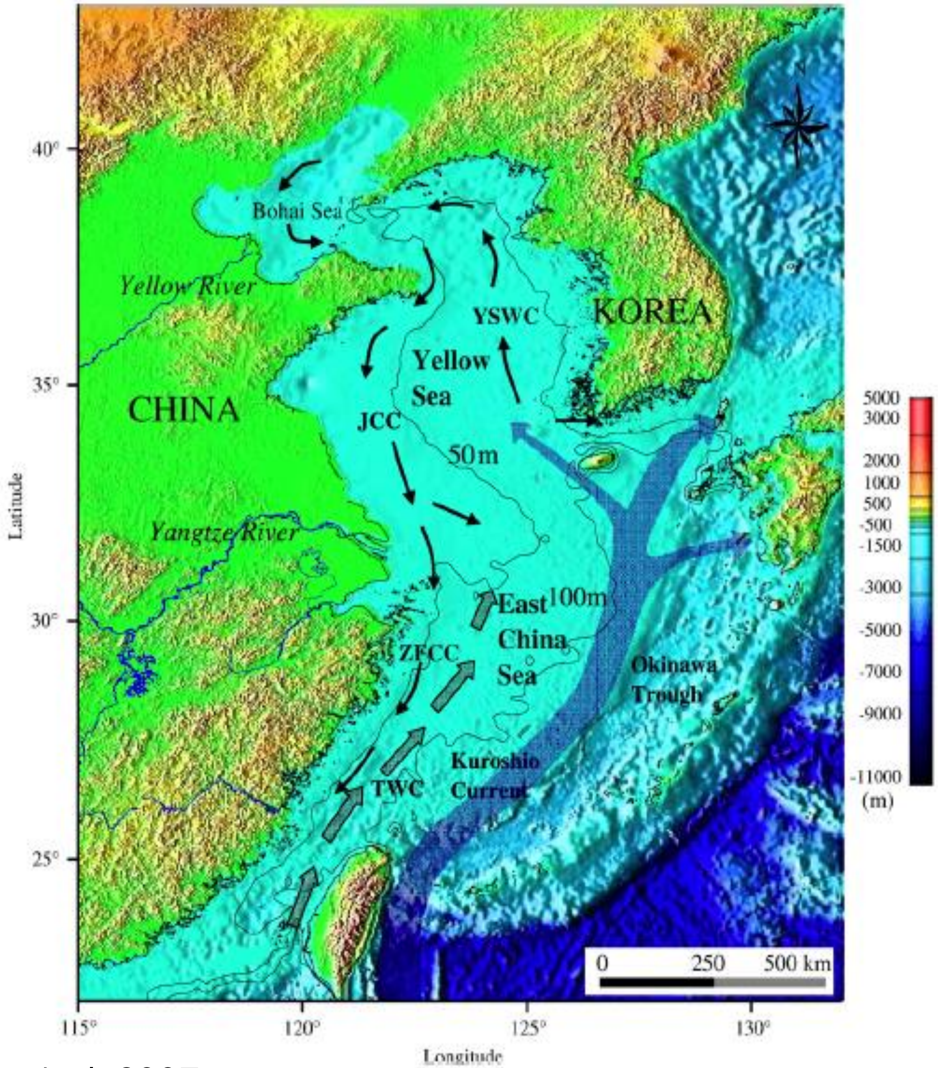

Liu et al. 2007

on pattern in the East China Sea and Yellow Sea. JCC (Jiangsu Coastal Current); TWC (Tai
rent); YSWC (Yellow Sea Warm Current); ZFCC (Zhejiang Fujian Coastal Current).

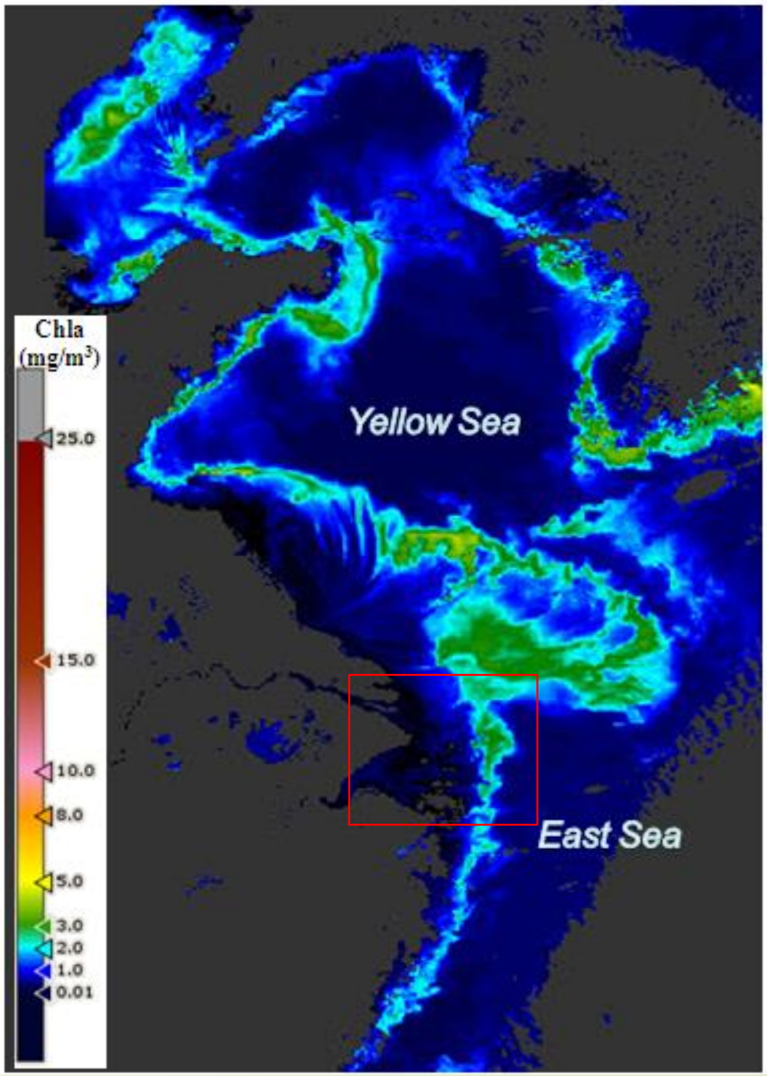

Algae bloom - macroalgae

- Green tides: *Ulva prolifera*

Floating Algae Index (FAI) (Hu et al., 2010).

$$R_{rc,\lambda}(\theta_0, \theta, \Delta\phi) = \pi L_{t,\lambda}^{*}(\theta_0, \theta, \Delta\phi)/(F_{0,\lambda} \times \cos\theta_0) - R_{r,\lambda}(\theta_0, \theta, \Delta\phi),$$

$$\mathrm{FAI} = R_{rc,NIR} - R_{rc,NIR}',$$

$$R_{rc,NIR}' = R_{rc,RED} + (R_{rc,SWIR} - R_{rc,RED}) \times (\lambda_{NIR} - \lambda_{RED})/(\lambda_{SWIR} - \lambda_{RED}),$$

Bands: 645, 859, 1240 nm

Approximate location and distribution of *U. prolifera* identified from MODIS FAI imagery from April 2000 to May 2009.

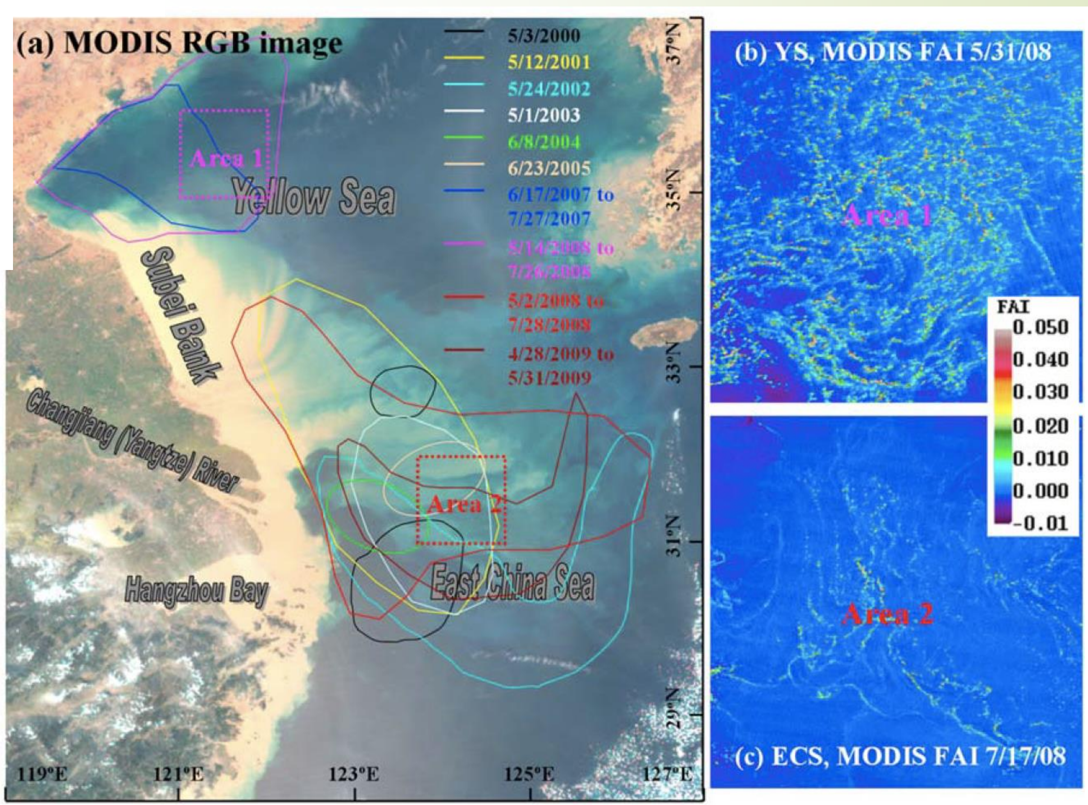

Algae bloom - macroalgae

- Brown tides: *Sargassum horneri*

Alternative Floating Algae Index (AFAI) (Qi et al., 2017).

$$\mathrm{AFAI} = R_{rc,\lambda 2} - R'_{rc,\lambda 2}.$$

$$R'_{rc,\lambda 2} = R_{rc,\lambda 1} + \left(R_{rc,\lambda 3} - R_{rc,\lambda 1}\right)(\lambda_2 - \lambda_1)/(\lambda_3 - \lambda_1),$$

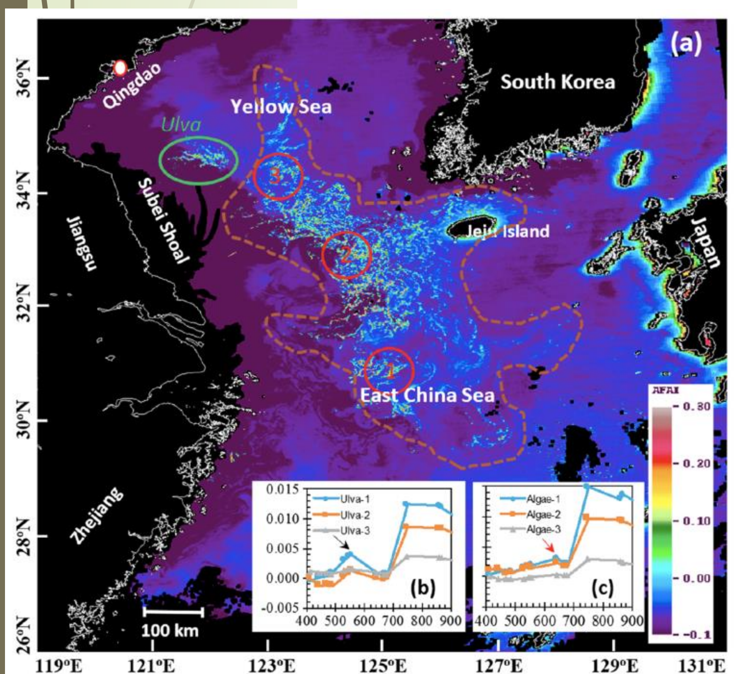

(a) MODIS AFAI image on 18 May 2017.

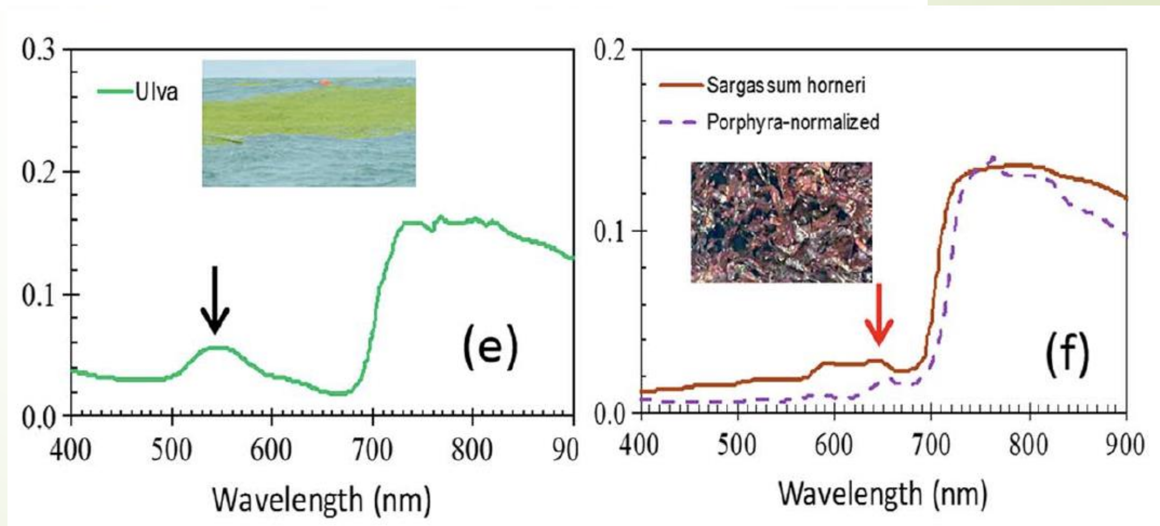

(e) Reflectance spectra of Ulva (Hu et al., 2015).
(f) Reflectance spectrum of Porphyra (inset photo), together with the S. horneri spectrum from Jin et al. (2016).

Algae bloom - microalgae

- Red tides:

Harmful algal blooms

Red tide Index (RI)

$$RI = \frac{[L_w(510)/L_w(555) - L_w(443)]}{[L_w(510)/L_w(555) + L_w(443)]}$$

(Ahn & Shanmugam 2006)

SeaWiFS detection in the BS and YS

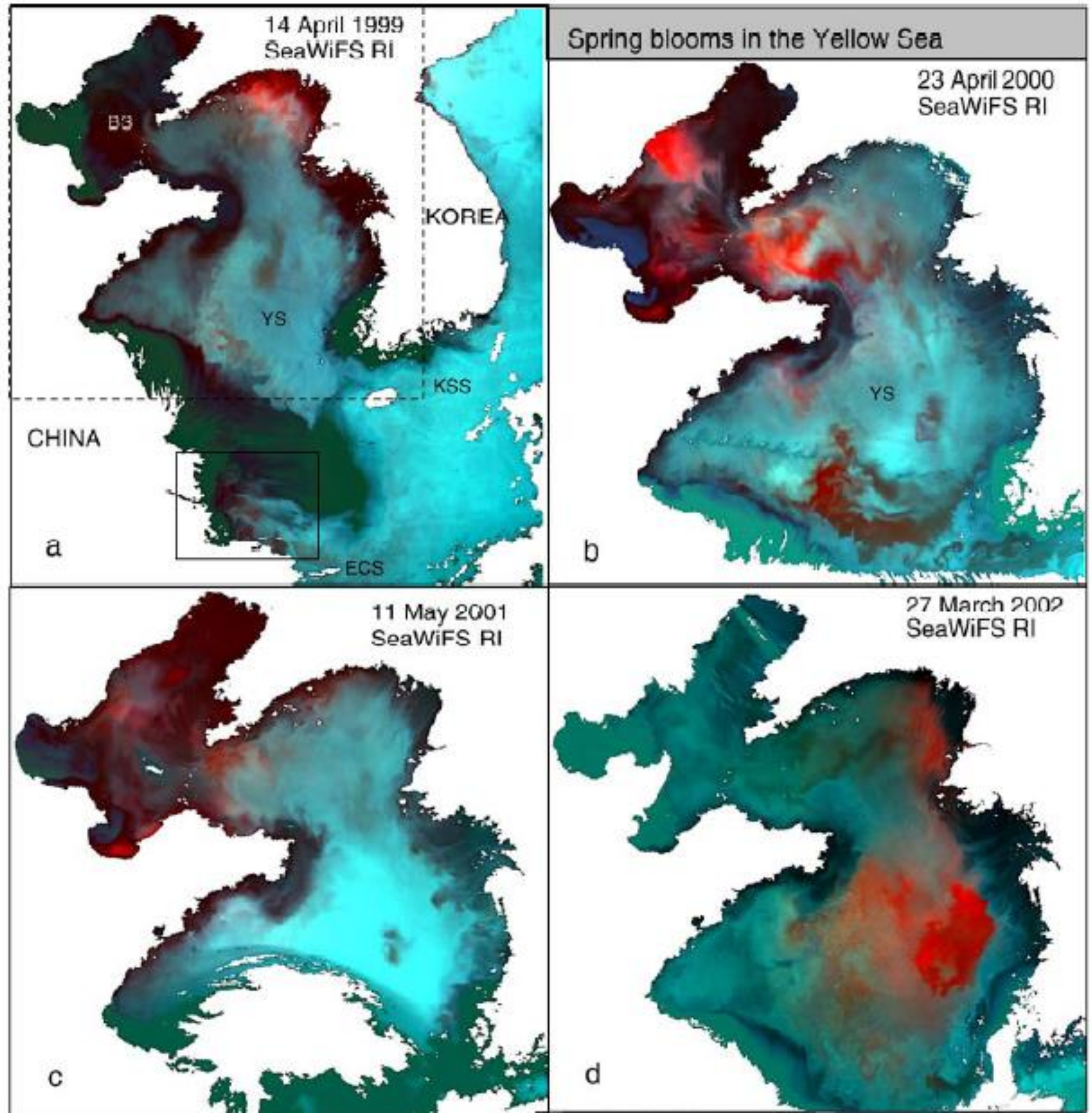

Algae bloom - microalgae

- Red tides: *Prorocentrum donghaiense* in the ECS using GOCI (Lou and Hu, 2014).

$$RI = \frac{R_{rs}(555) - R_{rs}(443)}{R_{rs}(490) - R_{rs}(443)}.$$

$$R_{rc} = \frac{\pi L_t^*}{F_0 \cos \theta_0} - R_r$$

$$nR_{rc} = R_{rc} - \Delta R_{rc}.$$

Modified Red tide Index (RI) using the normalized Rrc data at 443, 490 and 555 nm.

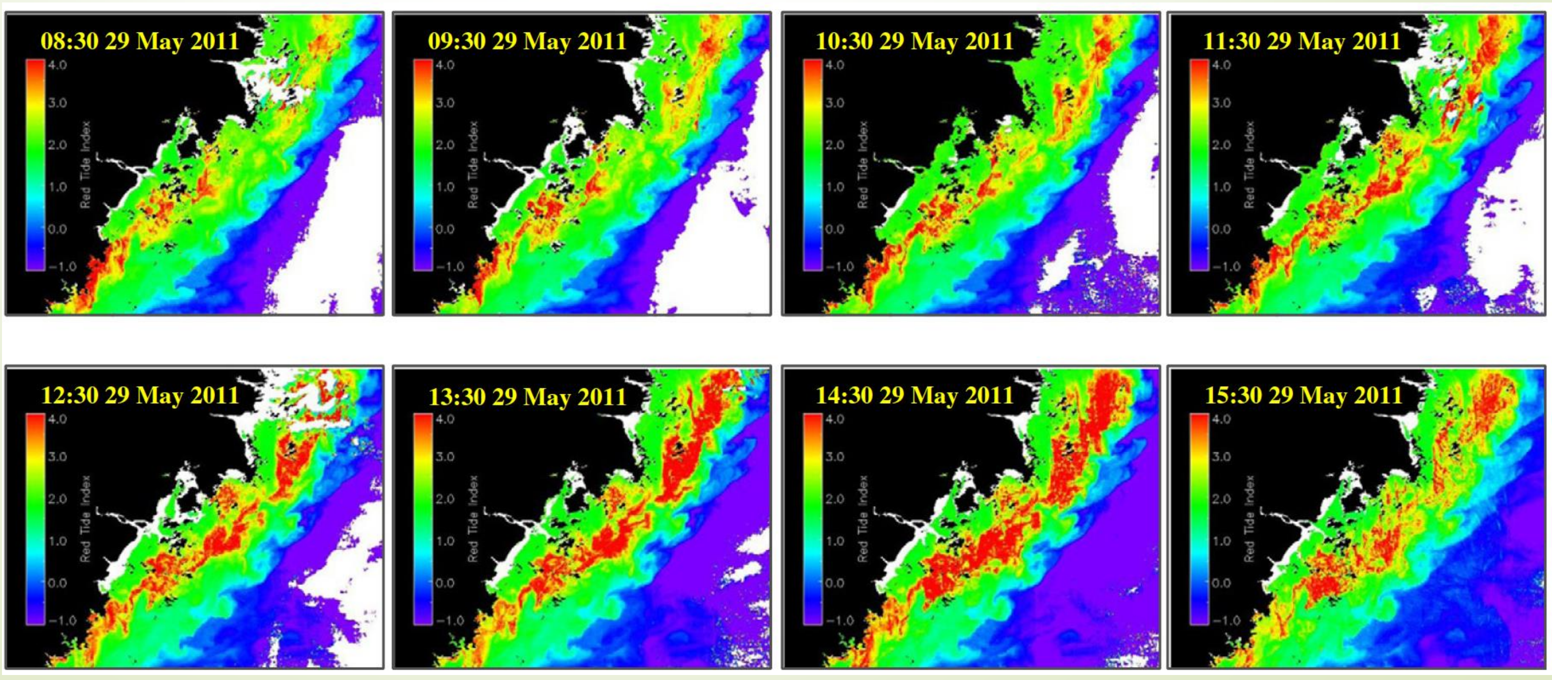

GOCI RI images for each hour

Algae bloom - microalgae

(Tao et al. 2015)

- Red tides:

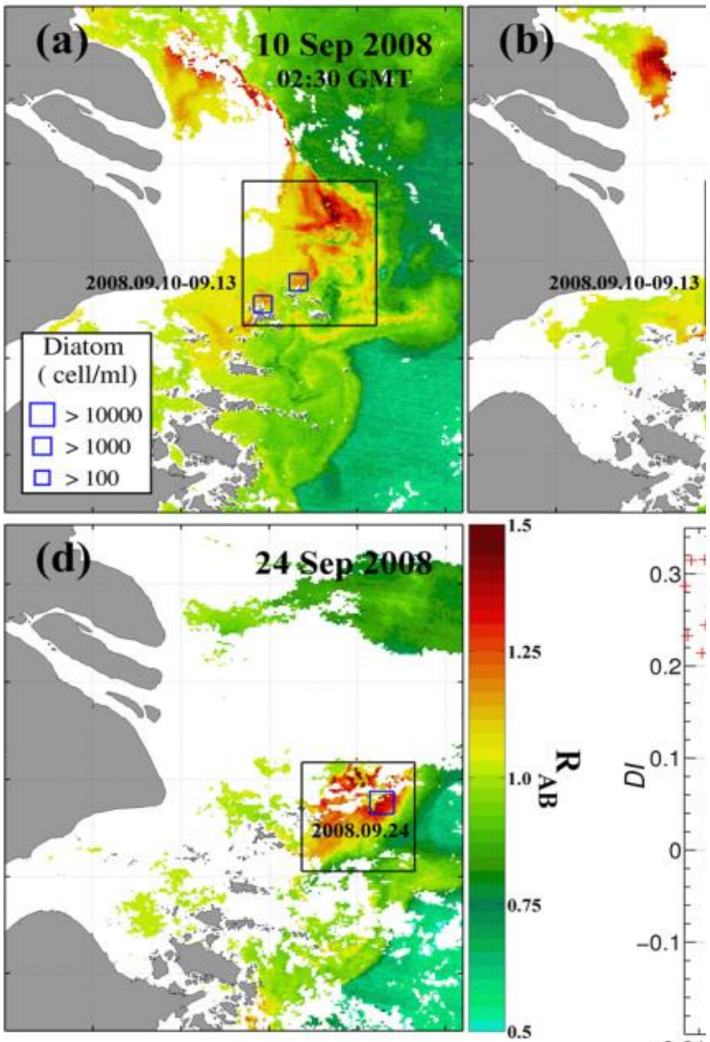

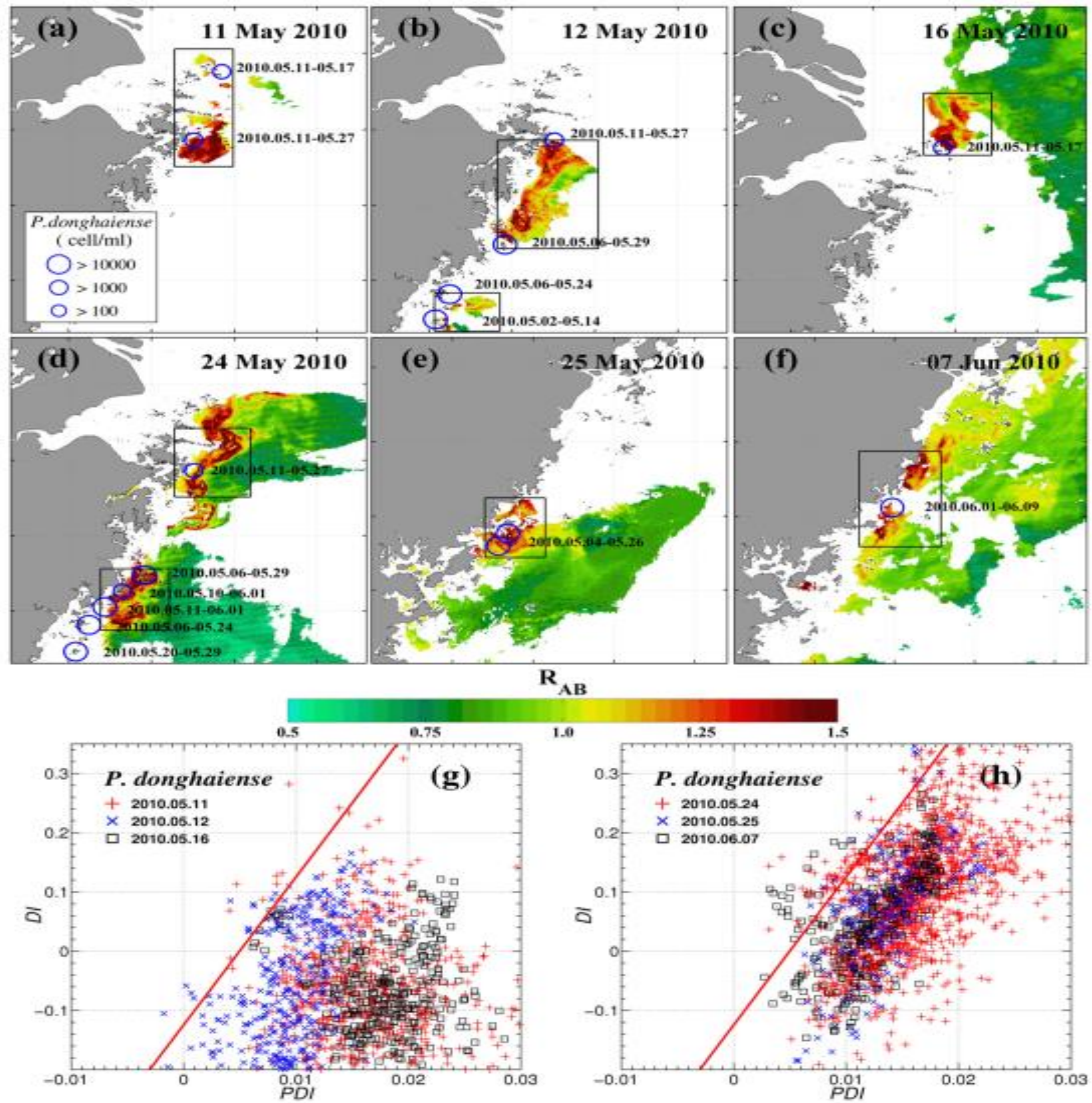

Phytoplankton size classes

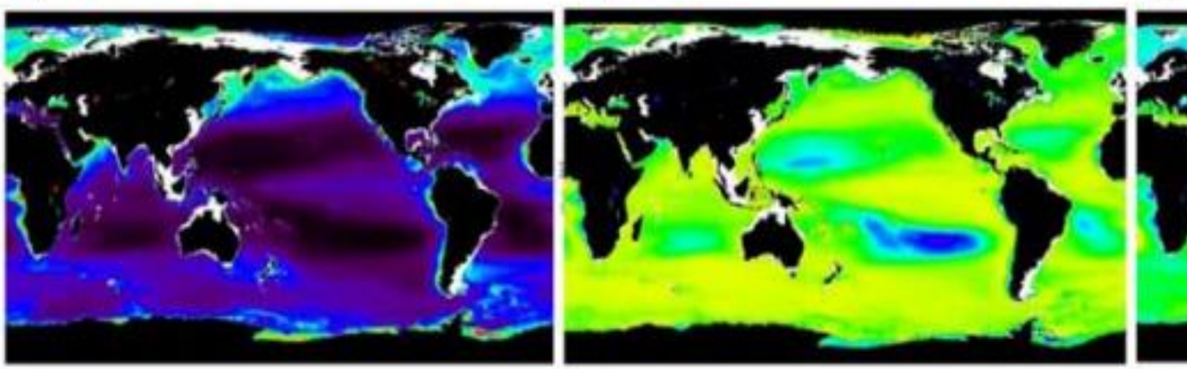

PSCs over 1998-2009 derived from SeaWiFS (a) Microplankton (>20μm), (b) N
and (c) Picoplankton (<2 μm), Hirata et al. (2011

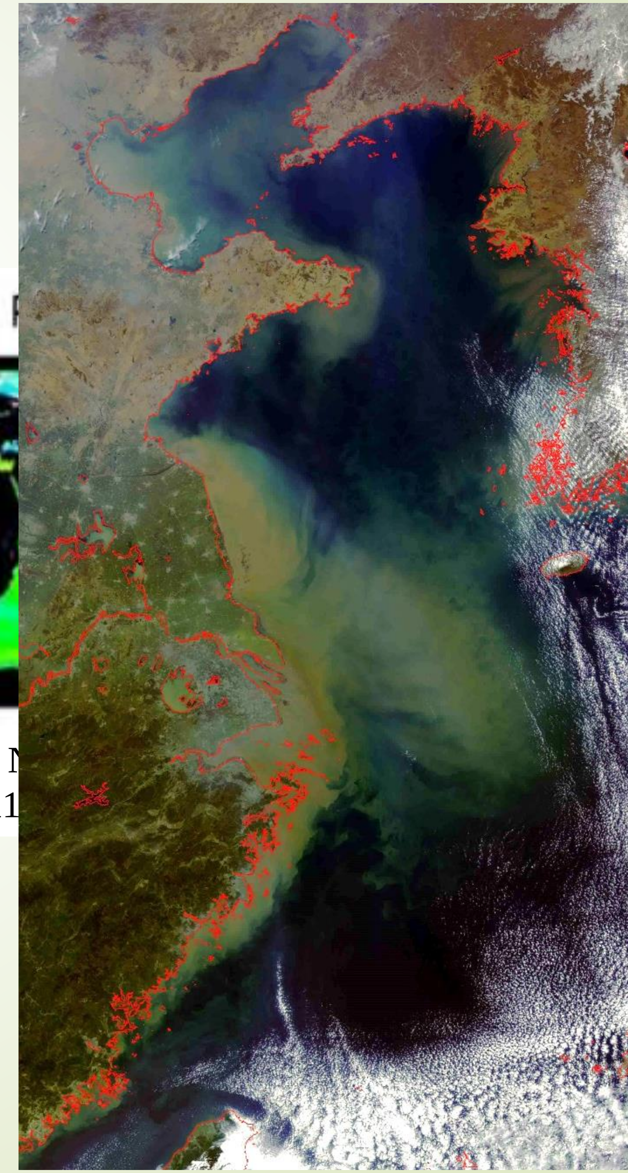

Phytoplankton size class

GOCI-derived Phytoplankton Size Classes (PSCs) diurnal variation, based on Abundance-based approach (HPLC pigments vs. PSCs)

(Sun & Shen et al. 2018 JGR)

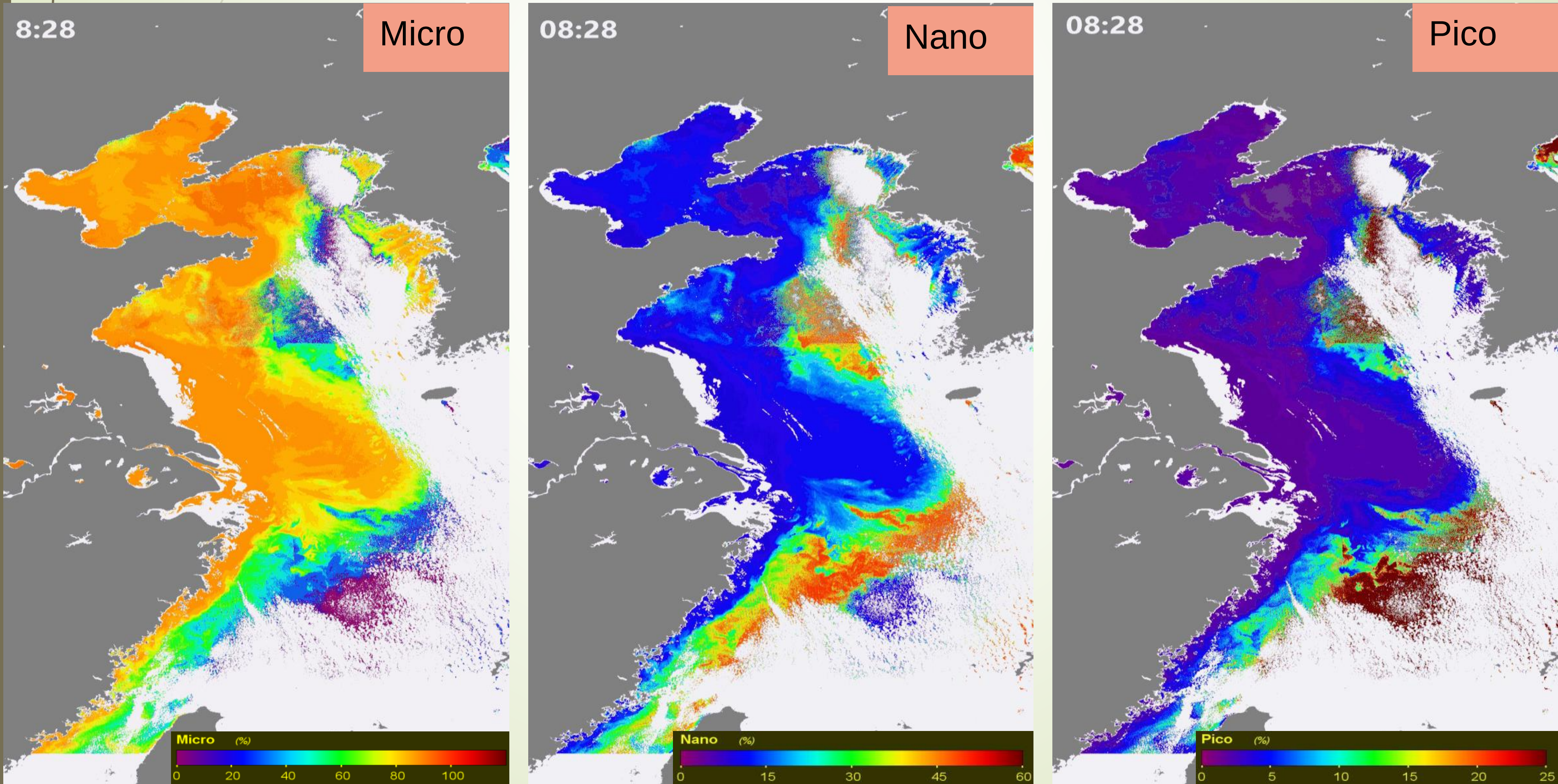

Phytoplankton species

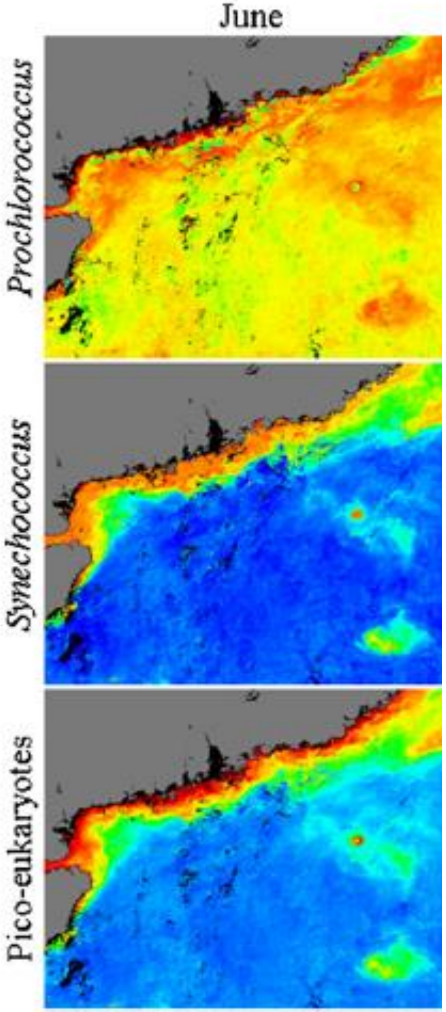

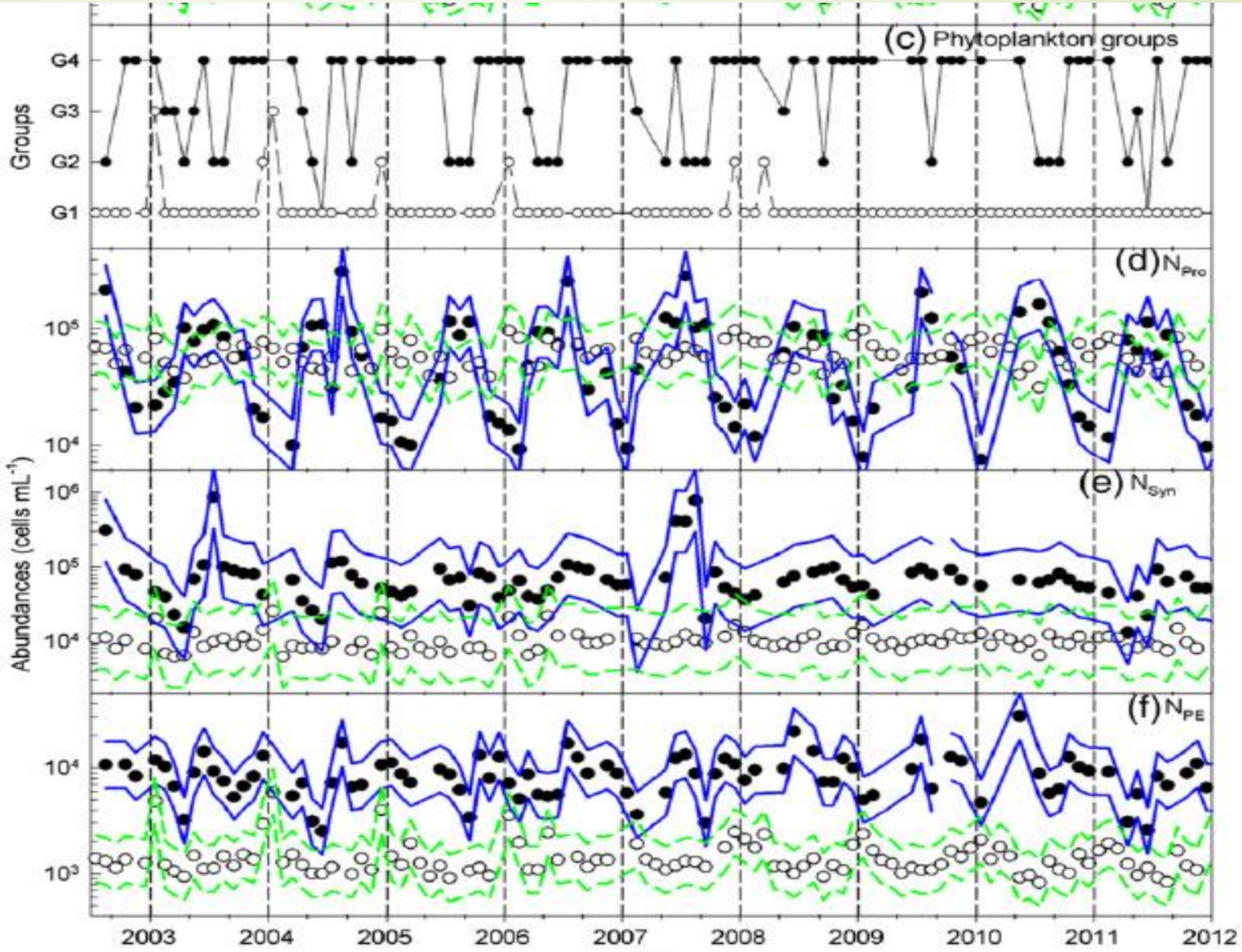

MODIS-Aqua derived monthly distributions of the cell abundances (in 10^5 cells mL−1) of Prochlorococcus原绿球藻, Synechococcus聚球藻, and pico-eukaryotes真核生物 in the NSCS in June and December 2009.

(Pan XJ et al 2013)

Applications in estuarine, coastal and shelf zones

- Sediment dynamics
  - Suspended sediment concentration (SSC)
  - Annual/seasonal/diurnal variation (surface)
  - Vertical variation (SPM transportation model combined)
  - High spatial and temporal resolution
- Phytoplankton dynamics
  - Chlorophyll-a concentration
  - Harmful Algal Blooms (macro- and micro-algae)
  - Phytoplankton size class
  - Phytoplankton species
- Optical and Thermal joint data

Optical & Thermal data for coastal oceans

- Water mass
- Front
- Eddy
- Upwelling
- Climate Change

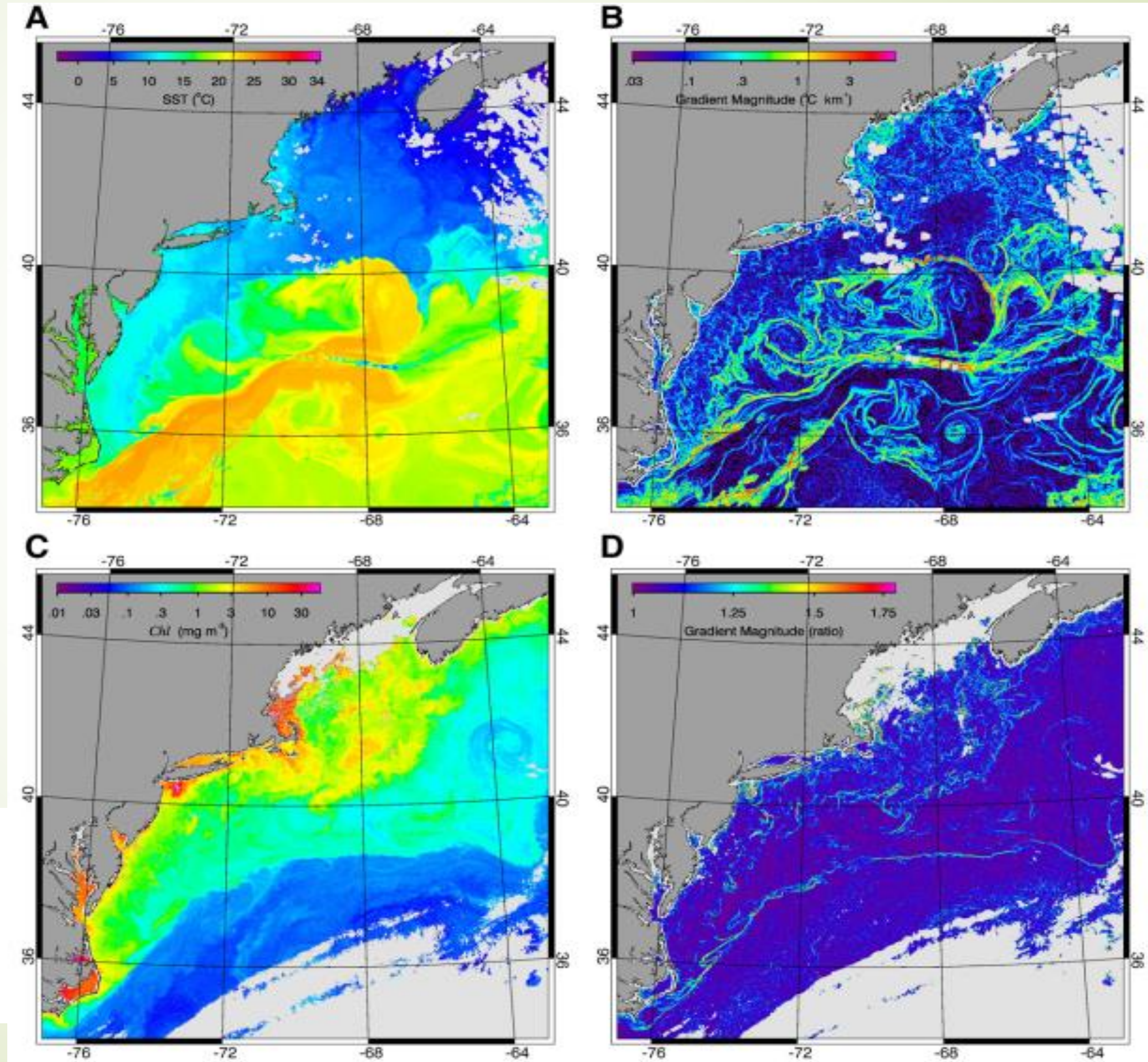

Oceanic front detection in Chl and SST satellite imagery in Gulf of Maine and Georges Bank. (Belkin & O'Reilly, 2009).

Optical & Thermal data for Eddy vs. Chla

Cold eddy & enhanced Chla coincident

(Alpers et al. RSE 2013)

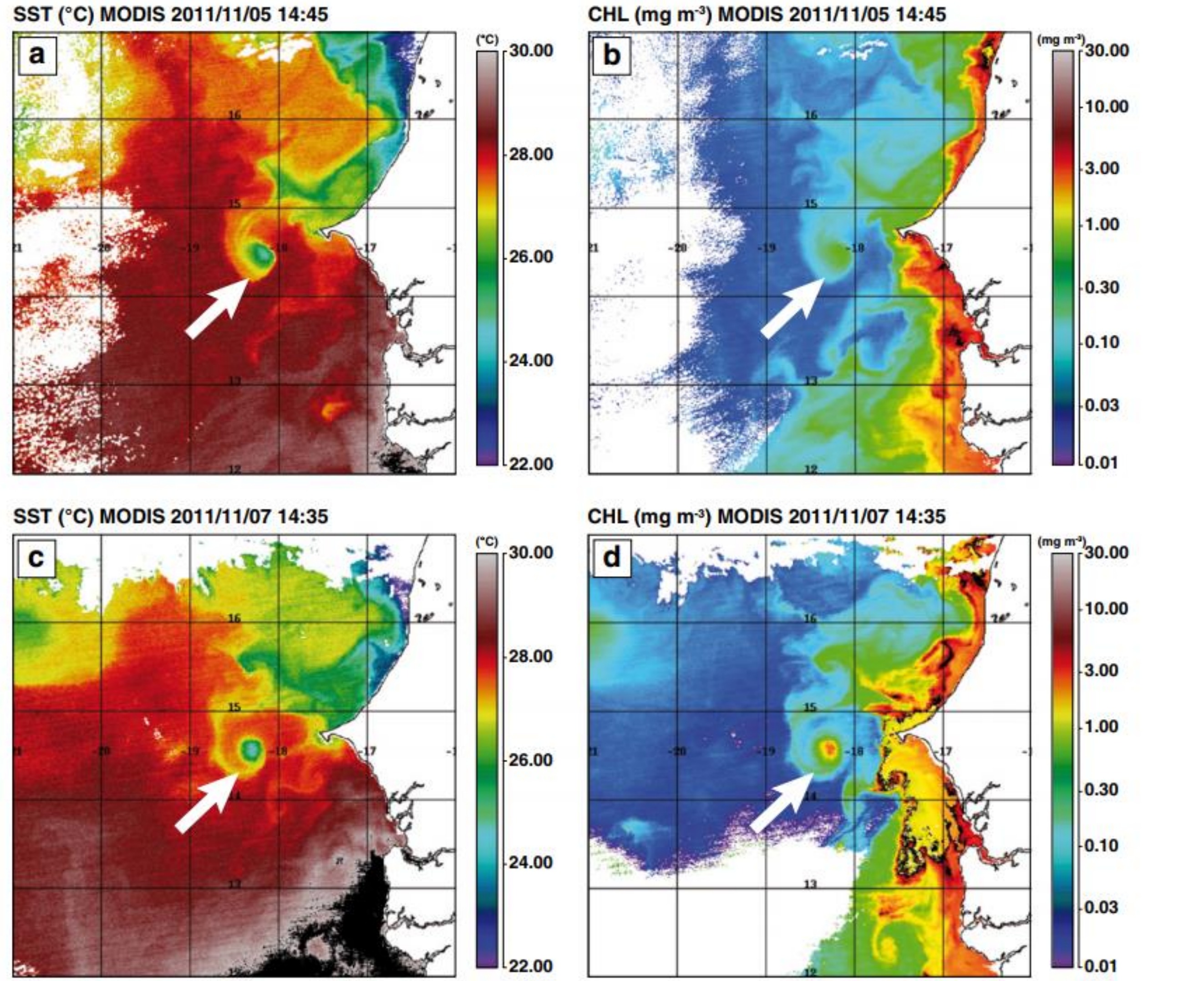

Fig. 6. Maps of the SST in degrees C and of the chlorophyll-a (CHL) concentration in mg/m^3 retrieved from MODIS data. Upper maps: at 1445 UTC on 5 November 2011. Lower maps: at 1435 UTC on 7 November 2011. The arrows point to the SST and CHL signatures of the small-scale eddy.

Optical & Thermal data for Fronts (SST vs. Chla)

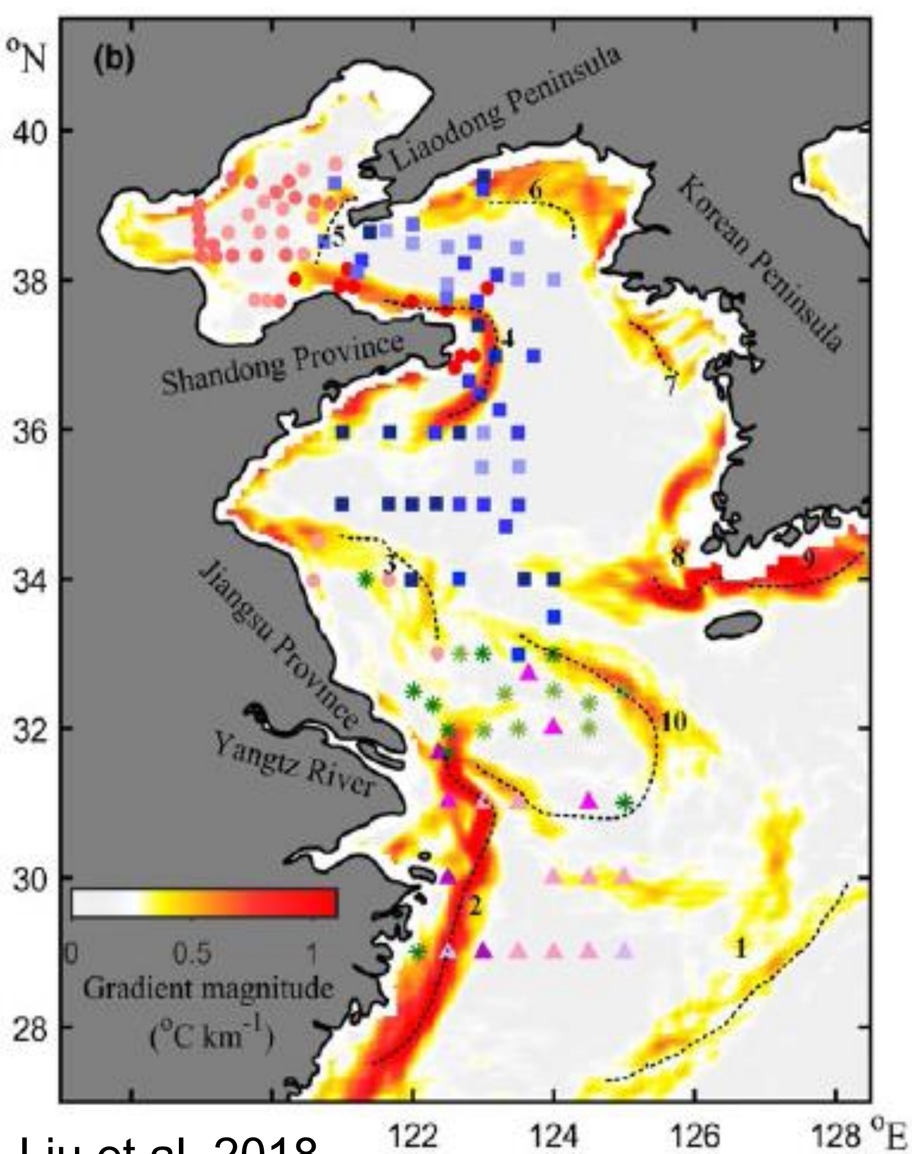

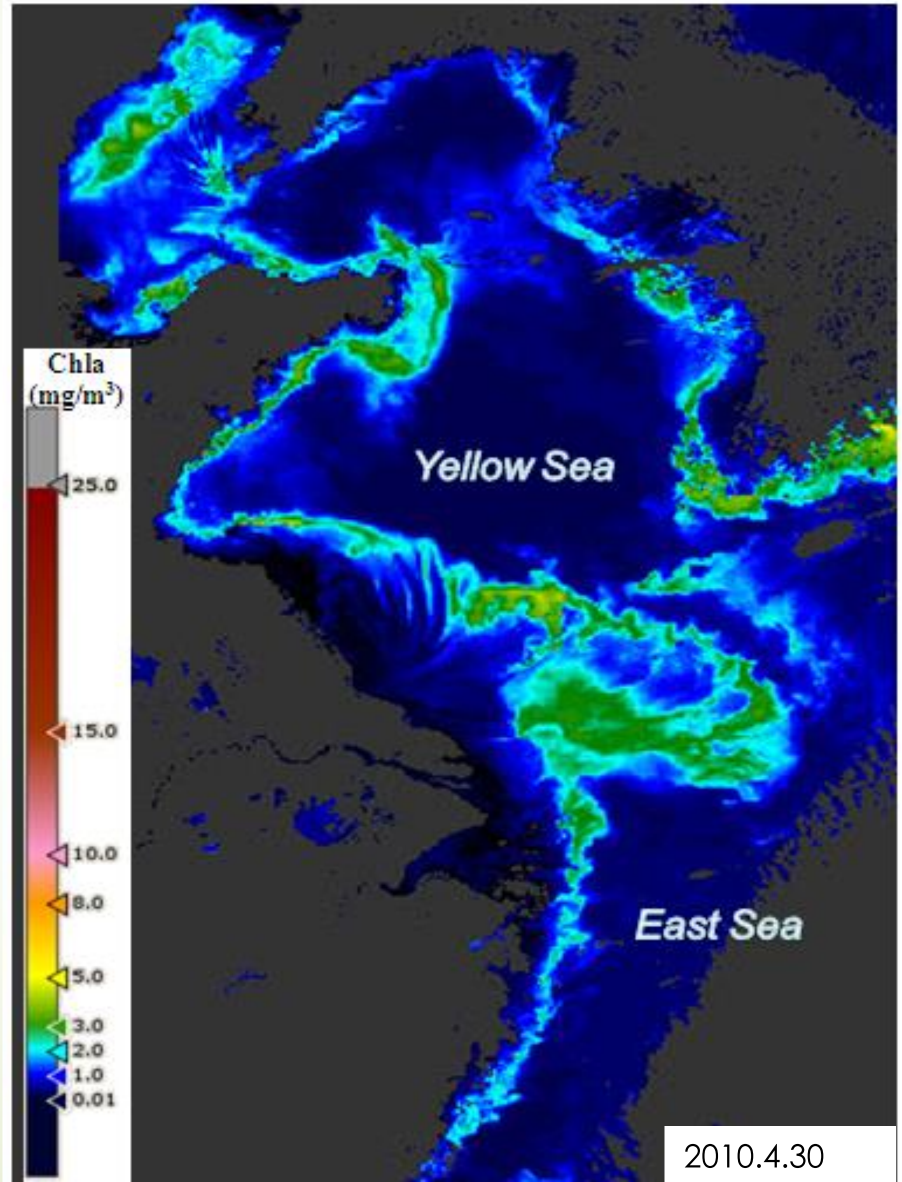

Liu et al. 2018

Optical & Thermal data for Fronts vs. phytoplankton microfossil

- Fronts partitioned phytoplankton microfossils into assemblage types of diatoms, dinoflagellates and Silicoflagellates in the BS, YS, ECS

(Liu et al., 2018 GE&B)

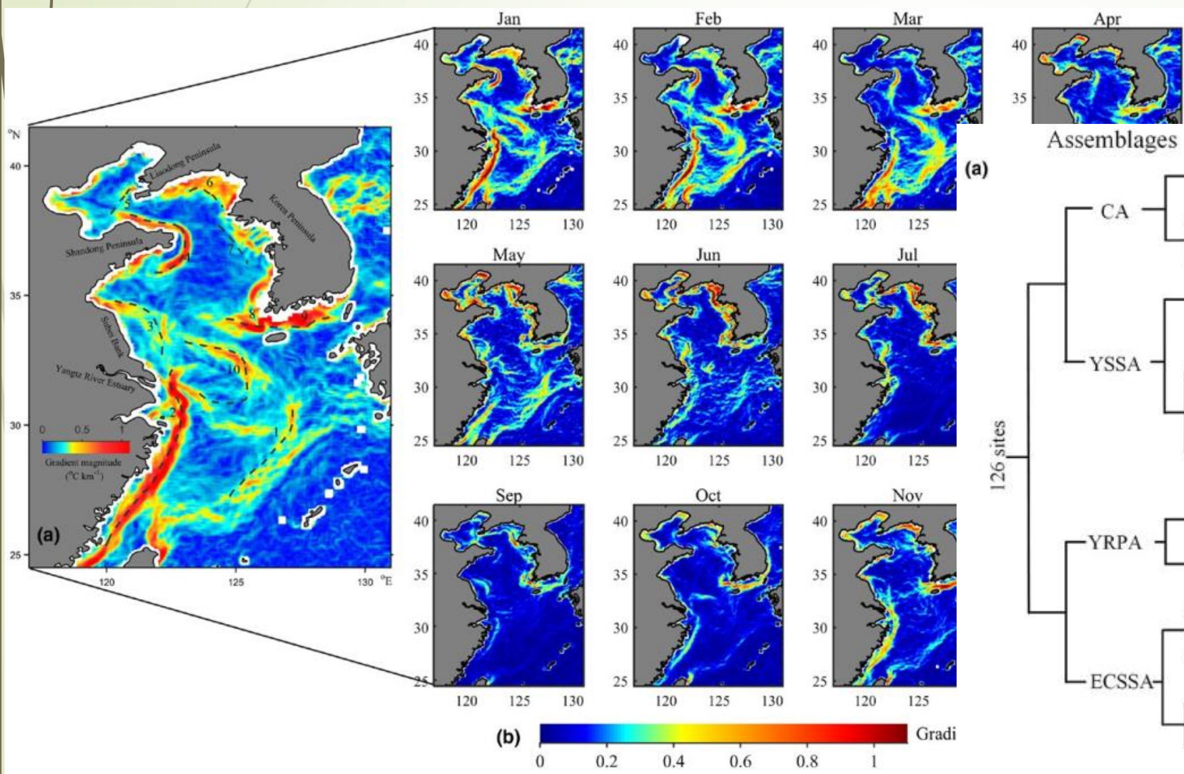

An integrated frontal map produced by monthly climatological SST mean from MODIS/Aqua images).

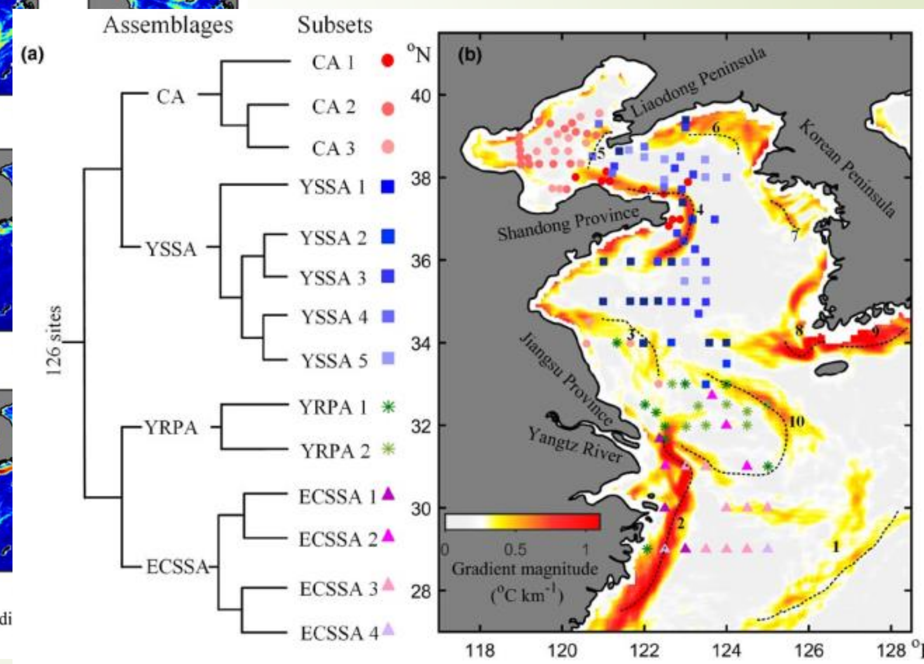

Classification of microfossil assemblages from a two-way indicator species (b) Geographical map of microfossil assemblages coupled with front patterns

Applications in estuarine, coastal and shelf zones

What else can we explore further using Remote Sensing technology for applications? (trend of 3-H)

- Hyperspectral

  GaoFen-5, EnMap (Germany), HyspIRI(US), …..

- High-spatial resolution

  GaoFen-1/2/6, Sentinel-2A/2B, ….

- High-temporal resolution

  GOCI-1/2, Geo-CAPE?, OCAPI?……

Thank you for your attention!

fshen@sklec.ecnu.edu.cn